Journal for Occultation Astronomy

Volume 16 · No. 3 2026-03

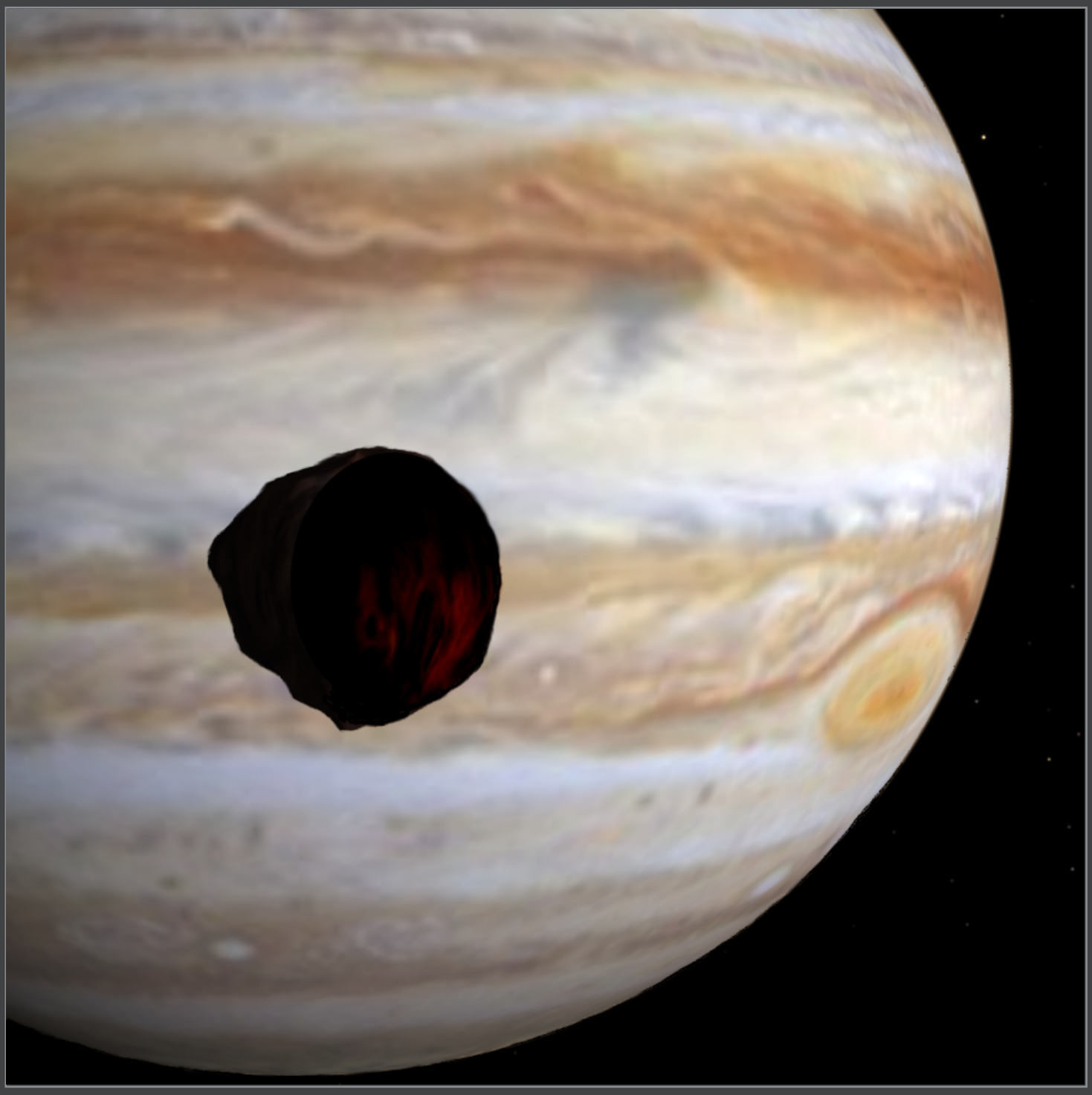

Mutual Phenomena of Jupiter's Satellites Amalthea and Thebe

Dear reader,

Every six years many of us record the mutual eclipses and occultations of Jupiter's Galilean satellites. The next PHEMU campaign has begun. More valuable, but more difficult, are when they or Jupiter eclipse the inner moons Amalthea and Thebe. Read how to observe them and submit data to Paris Observatory.

On August 12 Europe will experience another total solar eclipse. It occurs near sunset and Mariusz Krukar describes how the twilight sky will be affected by the extended umbra, and how to make valuable observations.

The European project to observe lunar occultations of double stars (OLED) is attracting more observers. Enrique Velasco (ES) and Philippe Laurent (FR) present an overview of its methods and results, and invite the worldwide IOTA community to take part. In addition, Nikolai Wünsche discusses high-speed photometry of lunar occultations.

Discovered an asteroidal satellite? Dave Herald *et al* give a protocol to follow to support your claim.

Clear skies,

Alex Pratt
IOTA/ES

COVER

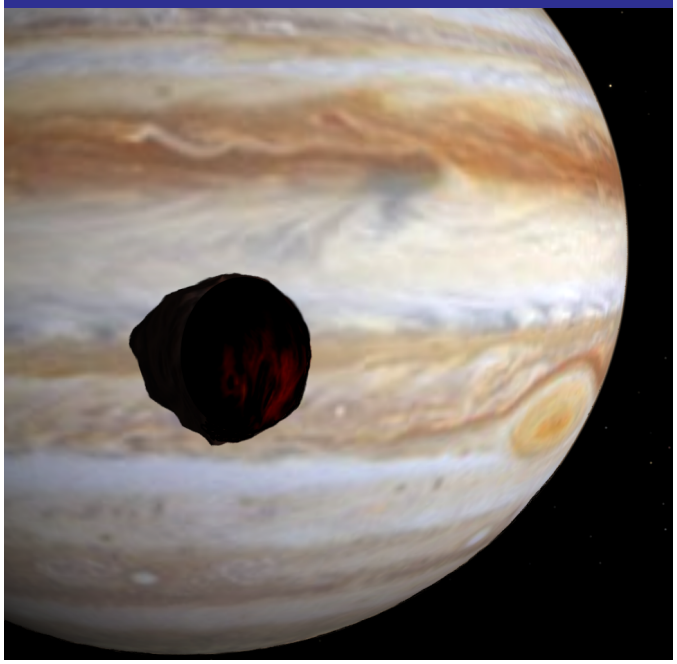

The cover image shows an artist's impression of Jupiter's satellite Amalthea during its eclipse by Callisto on 2026 November 8. The challenging observation of the eclipse is part of the Phemu campaign 2026/2027. In addition, eclipses of moon Thebe by the Galilean satellites can be observed. A Call for Observations in this issue explains how these difficult measurements can be carried out. (Graphic: Celestia 1.6.2.2., image processing: O. Klös)

JOA Volume 16 · No. 3 · 2026 -3 $ 5.00 · $ 6.25 OTHER (ISSN 0737-6766)

In this Issue:

Copyright Transfer

Rules for Authors

In order to optimise the publishing process, certain rules for authors have been set up how to write an article for *JOA*. They can be found in "How to Write an Article for *JOA*" published in this *JOA* issue (2018-3) on page 13. They also can be found on our webpage at https://www.iota-es.de/how2write_joa.html .

Journal for Occultation Astronomy

CALL FOR OBSERVATIONS:

Eclipses of Amalthea and Thebe by the Galilean Satellites and by Jupiter

Jean-Eudes Arlot · LTE[1] · Observatoire de Paris · Paris · France · phemu.imcce@obspm.fr
Thierry Midavaine · Club Eclipse · SAF[2] · Gemini ProAm · Paris · France · thierrymidavaine@sfr.fr
Michael Irzyk · Planète Sciences – TJMS Observatory · SAF[2] ·Buthiers · France · irzyk.michael@gmail.com
(1) Laboratoire Temps Espace, (2) Société Astronomique de France

ABSTRACT: The PHEMU (mutual phenomena) campaign is one of the oldest periodic ProAm collaborations proposed to the worldwide amateur community. About every 6 years, occultations and eclipses between the Galilean satellites provide very easy events to catch with small telescopes. Same synchronised phenomena could be observed from the hemisphere of Earth with Jupiter above the horizon. It enabled the improvement of ephemerides of these satellites which were the targets of space probes. These ephemerides now meet high accuracies thanks to these space missions or exceptional stellar occultations. Small inner Jupiter satellites could be the target of amateurs to improve their respective ephemerides. It will allow us to place constraints on the radial density distribution inside Jupiter. These events are more difficult to catch. However, previous recordings and trials performed with new sensitive digital cameras demonstrate selected events are now in the range of amateur abilities. This paper is introducing the 2026 - 2027 campaign to the amateur community able to deal with telescope availability, longitudes and weather constraints. In the coming year, amateurs have dates with the best eclipses of Amalthea and Thebe close to when Jupiter is at quadratures. Paris Observatory LTE is waiting for your accurately time-stamped light curves!

Introduction

Since 1973, every six years for about one year, the mutual phenomena of Jupiter's moons have provided a rendezvous between observers and celestial mechanics. These observations have greatly contributed to improve our understanding of the dynamics of Jupiter's moons and their ephemerides [1], [2]. The last observation campaign took place in 2021, and another campaign is being planned for 2026-2027.

The Galilean moons are celestial bodies well known to all observers. They have always been a favourite of researchers, and even more since they became a target for space probes. They are fast-moving bodies perturbed by the Sun, the oblateness of Jupiter and Saturn, and also by each other. These characteristics make them a solar system in miniature, where certain poorly understood effects can be observed more quickly. Curiously, they are not the most frequently observed bodies in the solar system, even though they are among the brightest. In fact, it is their magnitudes (they are too bright!) that hinder their observation and, to measure their positions, we have often used the observation of their eclipses by Jupiter or, better, their mutual eclipses and occultations (Figures 1a, 1b).

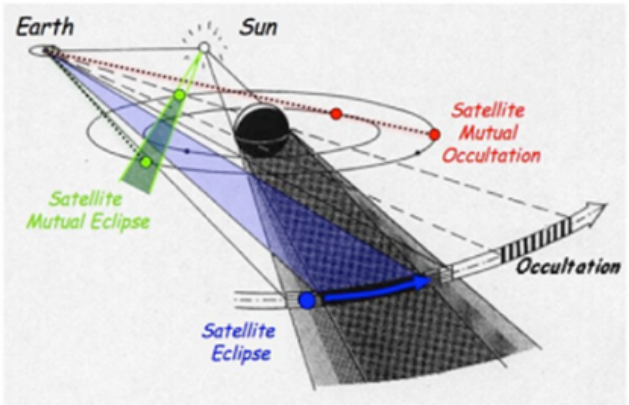

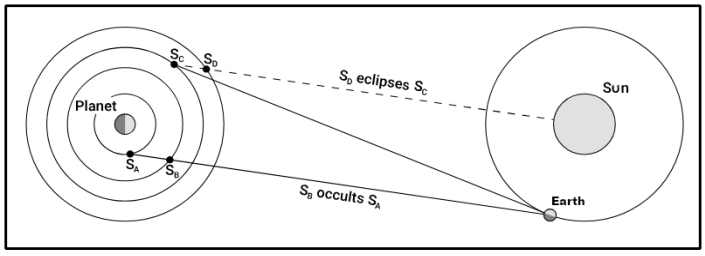

Figures 1a, 1b. The configurations allowing the phenomena of eclipses and occultations. The maximum angular shifts between Earth and Sun are met during the 2 quadratures, they bring the best conditions to catch the eclipsed satellite light curve.

Jupiter also has other moons, much smaller and less bright: a series of small bodies between Io and Jupiter, and another series beyond Callisto. The latter are easy to observe (Jupiter is far away and not troublesome), but the former, closer to the planet, are flooded in Jupiter's halo and difficult to detect. Yet, scientifically, a precise understanding of their motion can tell us about the actual nature of Jupiter. Our knowledge of the dynamics of these moons is still incomplete. For example, the accuracy of the ephemeris of Amalthea is on the order of 200 km, while that of the Galilean moons is about 30 km. This is why astrometric observations are encouraged, and, of course, so are observations of their eclipses. During the 2009 and 2015 campaigns, professionals and amateurs successfully recorded some events with 2 m, then 1 m and 60 cm telescopes [3], [4]. Thus, for the very favourable period of 2026-2027, we propose here a campaign to attempt observations of the eclipses of the small inner satellites Amalthea and Thebe by the Galilean satellites or by the planet Jupiter.

The 2026-2027 Occurrence

The period 2026-2027 is favourable for observing the mutual phenomena of Jupiter's moons : the planetocentric declination of the Earth and the Sun becomes zero (the Earth and the Sun are then in Jupiter's equatorial plane, which is also the orbital plane of the satellites) at a date close to Jupiter's opposition. The northern hemisphere is favoured, as Jupiter's declination is positive at these dates (Figure 2 and Table 1).

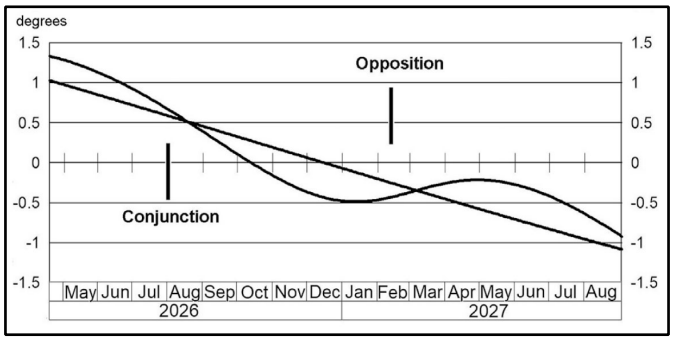

Figure 2. Planetocentric declination of the Earth and the Sun.

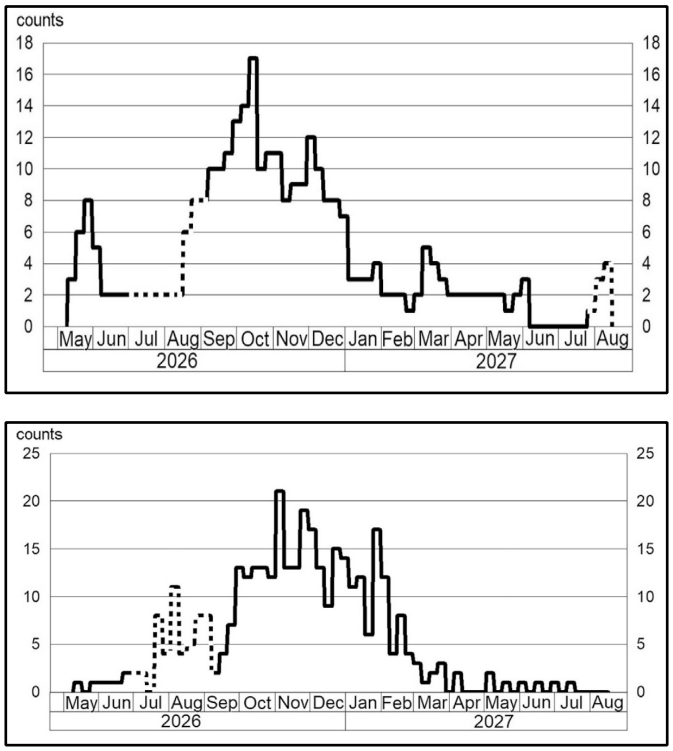

Figures 3a, 3b. The number of observable events (by week) of the Galileans (3a, top) and Amalthea and Thebe (3b, bottom). Dotted lines correspond to events too close to the conjunction of Jupiter and the Sun and so are unobservable.

Table 1 gives the key dates for observational conditions for the period 2026-2027: the best observations are made between opposition and quadrature, and the phenomena are more numerous near the equinox and when the Earth is in the orbital plane of the satellites.

Year	Date	Configurations
2026	April 5	Jupiter at quadrature
	May 11	Mutual events begin
	July 26	*Conjunction of Jupiter and the Sun*
	October 10	**Earth is in the orbital plane of the Galilean satellites**
	November 18	Jupiter at quadrature
	December 16	**Equinox on Jupiter**
2027	February 11	**Opposition of Jupiter**
	May 16	Jupiter at quadrature
	August 10	Mutual events end
	August 25	*Conjunction of Jupiter and the Sun*

Table 1. the observational conditions depend on key dates and defined time periods shown in Figures 3a and 3b.

Satellites	Periods of revolution	Eccentricities	Inclinations to Jupiter's equator (°)	Magnitudes at opposition	Maximum elongation at opposition
Amalthea J-5	11.956296 h	0.003	0.4	14.1	59 arcsec
Thebe J-14	16.188 h	0.015	0.8	15.7	73 arcsec

Table 2. Characteristics of Amalthea and Thebe.

The Satellites Amalthea and Thebe

Among the small inner satellites of the Jupiter system, we will limit our observations to the satellites Amalthea and Thebe because they are the brightest (magnitude 14 and 16) and therefore the most accessible even if their detection and observation remains a challenge.

We can see that these satellites always remain very close to the planet Jupiter. Therefore, they must be observed when they are close to their maximum elongation, but for observing eclipses, the timing is not a matter of choice. Amalthea is brighter but it is closer to Jupiter than Thebe. Therefore the ability to detect them are in the same range (Figure 6), in the most favourable conditions, with maximum elongations. Of course, we are not chasing transits or occultations of small satellites with Galilean satellites but only eclipses. The most interesting geometry to catch eclipses is around the quadrature periods (Figures 1a, 1b and 3b). This allows to get Amalthea and Thebe far from the eclipsing Galilean satellite while crossing its shadow. We may notice in Table 2, Amalthea's period is 11.956296 h, it is very close to the half Earth sideral period: 11.967146 h. Therefore, one night before an event or one Earth sideral period (23h56m04s) or two Amalthea periods around Jupiter, you get a similar geometry of the relative angular position of Amalthea vs Jupiter and a similar Jupiter angular line of sight (Azimuth and Elevation) in the sky from your observatory to train yourself, record and measure your SNR.

The Eclipses

These satellites undergo two types of eclipse: eclipse in the shadow of the planet Jupiter and eclipse in the shadow of a Galilean satellite.

- **Eclipses in the shadow of Jupiter**
  Jupiter's shadow is very large, and the satellites are very close. Therefore, there is an eclipse at each revolution of the moon around the planet. Unfortunately, all phenomena will not be easy to observe, why? It's important to note that such an eclipse corresponds to an alignment of the Sun, Jupiter, and satellite. Thus, from the Sun, we cannot observe such an eclipse, and unfortunately, viewed from Jupiter, the Earth is very close to the Sun, so the eclipse is hardly more visible from Earth than from the Sun. We must therefore wait until the Earth is as far from the Sun as possible, as seen from Jupiter, in order to have the eclipse occurring as far away from one side of the limb of Jupiter as possible. These are the periods close to the two quadratures, while opposition being the worst time! In addition, we have to remember that Jupiter's atmosphere gives a blurred shadow giving a gradual light curve attached to an eclipse.

- **Eclipses in the shadow of the Galilean satellites**
  The shadows produced by the Galilean moons are much smaller than Jupiter's, and for the occurrence of an eclipse, the Sun, the smaller moons, and the Galilean moons must be in the same plane. This happens around the equinox on Jupiter because all the moons are in Jupiter's equatorial plane. Eclipses can therefore occur whenever the Sun passes through this plane, which is during a period of several months around the equinox (every six years). For this campaign the events around the 18th of November will be the most favourable.

The Observation of Eclipses

Please, refer to the technical notes concerning the observational techniques for Jupiter satellites mutual phenomena [5], [6] and Saturn satellites mutual phenomena [7], [8]. However, there are some important differences compared to phenomena involving only the Galilean satellites:

- Observations are simpler because the photometry does not need to be absolute: it's an ON/OFF phenomenon. The flux drop does not need to be quantified and measured; it is total. The satellite is visible and disappears as it enters the umbra, more or less rapidly depending on the penumbra surrounding the satellite's shadow. The eclipse ends when the satellite emerges from the umbra and the penumbra. It is necessary to time – very precisely in UTC to better than 0.1 seconds – the entry and exit of the satellite from the shadow of the Galilean satellite that is eclipsing it; that is, the beginning and end of the eclipse (the timings are given in the predictions).

- Observations are more difficult because the satellites are magnitude 14 (Amalthea) and 16 (Thebe), and this occurs very close to the planet Jupiter, which floods the satellites in a halo that must be mitigated. Amalthea is the brightest and can be up to 59 arcseconds from Jupiter, or 34 arcseconds from the planet's bright limb. Thebe is the faintest but can be up to 72 arcseconds from Jupiter, or 47 arcseconds from the limb. Unfortunately, the eclipses do not necessarily occur at the time of elongation.

The observational methods will therefore differ from those used to observe the Galilean moons.

- **Faint objects**

  The faint magnitudes of the satellites will require the use of telescopes with a sufficient diameter to reach magnitude 14 for Amalthea (easy) and 16 for Thebe (difficult) with limited exposure to be above a minimum frame rate to improve timing resolution of the event. In previous recordings [4] rates were lower than 0.04 Hz for 20 s exposures. The eclipse monitoring was done for 15 min around the predicted event. Most of the event durations are in the range of 1 to 5 min except four events in the range of 13 min and 60 min. Again, we need to get your precise time-stamped light curve of the eclipse ingress and egress. Normally, a 30 cm telescope can detect an object of magnitude 14, but in our case, we need to record a fairly fast light flux drop, and we cannot integrate the light over too long a time for a wished 10 s exposure to be above 0.1 Hz (1 frame per 10 seconds). A 60 cm telescope is therefore much better suited. For Thebe, a 1 m telescope was necessary. Thanks to the sensitivity improvement of digital APS CMOS cameras have shown, the satellite could now come into the range of smaller telescopes. Very clean optics are an important requirement to record these events.

- **The presence of a bright Jupiter**

  The planet Jupiter is very bright, and Earth's atmosphere, along with optical scattering, propagates a halo of light over a great distance, enveloping the moons. They must be visible in order to unambiguously determine the timing of their disappearance into the shadow of the planet or another moon.

To observe these moons, it is important to observe from a site far from any light pollution, high above the horizon, with a sky free of even the slightest haze. The most troublesome source of light pollution is Jupiter's own. One way to reduce it is to use a methane (CH_4) filter, which darkens the planet's atmosphere by a factor of about 10 (Figures 4a and 4b) with a filter wavelength transmission bandwidth between 880 and 900 nm. The drawback is that this also reduces the amount of light from the satellite (though less than that from Jupiter's atmosphere, thus increasing the contrast) at the detector, requiring a more powerful telescope. This solution was successfully used by B. Christophe and O. Dechambre [4] with a 60 cm telescope in using an Edmund 890 nm, 10 nm bandwidth filter (Figure 9), in front an EMCCD Raptor Camera.

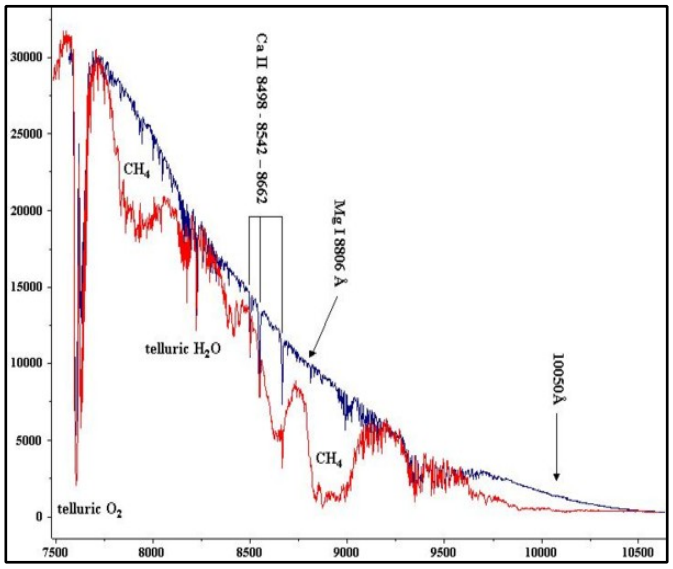

Figure 4a (top). Jupiter's atmospheric spectrum showing the CH_4 absorption bands. The absorption spectrum darkens the planet; the 890-900 nm band must be chosen, and a larger telescope is then required. (Observatorio Astronomica "G.V. Schiaparelli" Spettrometria, [9])

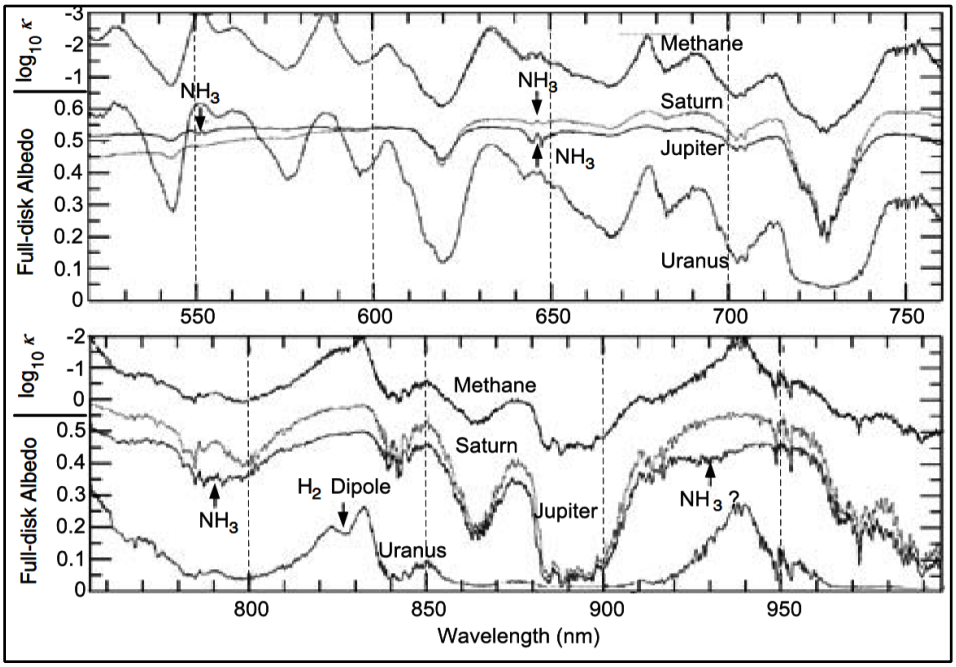

Figure 4b. Full disk albedo spectrum of Saturn, Jupiter and Uranus showing the 880 – 900 nm Methane absorption band. (from M. Mohler, J. Bühl et al. Exp Astron, [10])

Another way will be to put a mask in front of the focal plane on the detector cover glass or the camera window. The size of the mask is fitted to the defocused image size of Jupiter, in order to block the glare from the planet and to detect the satellite outside of the mask. A sharp edge alumina ribbon or a black velvet-like coated ribbon could be an effective solution. Figure 6 shows an image made by F. Colas at Pic du Midi with the 1 m telescope [4].

These methods need many training runs before the occurrence of the phenomena to allow you to tune exposure time, then frame stacking to measure your effective SNR (Signal to Noise Ratio).

- **When could we observe?**
  Observations of Amalthea's (or Thebe's) eclipses in the shadow of Jupiter must be made when these bodies are at the greatest possible angular distance from Jupiter's limb. The most observable planetary eclipses will be those occurring near quadratures, but even then, the distance from Jupiter's limb will be a maximum of 8 arcseconds for Amalthea and 10 arcseconds for Thebe.

Mutual eclipses, that is, eclipses of Amalthea and Thebe by a Galilean moon, are far more favourable in every respect: from an astrometric point of view, the connection with the eclipsing object is much more precise than with Jupiter's shadow (Galilean moons have no atmosphere), and from an observational point of view, the distance to the planet's limb is greater (however, note that the eclipsing satellite can be close to the small eclipsed satellite, and the difference in magnitude is significant (14 or 16 for small moons and six for Galilean moons). The distance to the Jupiter limb can reach 40 arcseconds. Table 3 lists the eclipses of Amalthea that are easiest to observe from Paris (and throughout France), and Table 4 lists those of Thebe.

From the web sites [11] you may compute the inner satellite events from your observatory, and the web sites [12], [13], [14], [15] and [16] you may get all the data related to Galilean satellites and useful data to prepare your campaign.

Observatory N: 007 - Paris
Timescale: UTC.

Mutual events of satellites J1, J2, J3, J4 eclipsing J5:

Date	begin: h	m	s	end: h	m	s	Type	Dur(m)	Impact	m	Δm	limb(")	dist(")	Planet(º)	Sun(º)	Moon phase
2026 11 8	2	55	50	4	3	28	4E5	67.6	0.999	14.69	-	27.24	86.71	33.783	-38.022	0.076
2026 11 10	4	44	58	4	47	48	1E5	2.8	0.184	14.67	-	26.69	21.56	49.509	-20.771	0.066
2026 11 17	5	20	41	5	22	41	1E5	2.0	0.134	14.63	-	11.16	27.28	54.019	-16.446	0.484
2026 11 26	3	7	13	3	10	23	1E5	3.2	0.166	14.57	-	29.12	21.35	44.535	-40.108	0.879
2026 12 3	3	47	20	3	49	25	1E5	2.1	0.105	14.53	-	14.52	27.09	51.602	-34.856	0.369
2026 12 10	2	35	45	2	39	59	3E5	4.2	0.384	14.48	-	23.72	56.27	47.128	-47.415	0.070
2026 12 12	1	27	28	1	31	4	1E5	3.6	0.293	14.47	-	31.02	19.38	39.115	-57.273	0.184
2026 12 19	2	13	57	2	16	6	1E5	2.1	0.129	14.43	-	17.57	24.55	48.705	-51.742	0.627
2026 12 24	5	10	17	5	12	51	1E5	2.6	0.420	14.39	-	22.79	20.03	49.855	-23.813	0.975
2026 12 27	23	44	5	23	48	40	1E5	4.6	0.292	14.37	-	32.01	15.50	33.321	-64.594	0.697
2027 1 4	0	40	39	0	42	54	1E5	2.2	0.109	14.34	-	20.29	19.41	45.748	-62.620	0.230
2027 1 9	3	34	57	3	37	32	1E5	2.6	0.080	14.31	-	21.47	15.92	52.713	-39.840	0.079
2027 1 12	21	51	29	21	59	15	1E5	7.8	0.223	14.30	-	30.91	9.93	26.375	-52.808	0.309
2027 1 14	23	1	11	23	6	48	3E5	5.6	0.096	14.29	-	29.75	31.92	38.767	-60.097	0.442
2027 1 19	23	7	36	23	9	58	1E5	2.4	0.100	14.27	-	22.58	11.84	42.956	-59.510	0.801
2027 1 25	2	1	29	2	3	22	1E5	1.9	0.632	14.26	-	20.07	9.21	54.784	-52.030	0.802
2027 2 19	19	20	1	19	25	7	3E5	5.1	0.821	14.25	-	33.89	11.82	30.151	-20.575	0.912
2027 3 21	2	56	24	3	47	18	1E5	50.9	0.974	14.35	-	30.18	12.06	16.062	-28.017	0.904

Table 3 .The best eclipses of Amalthea observable in France and in Europe (calculations made for Paris)
Legend:
Dur(m) is the duration of the eclipse in minutes
Impact corresponds to the minimum distance between the satellite and the centre of the shadow (0 for the centre, 1 for the radius of the eclipsing satellite)
m is the magnitude of Amalthea
limb(") is the angular distance from Amalthea to the limb of Jupiter in arcsec
dist(") is the angular distance from Amalthea to the eclipsing satellite in arcsec
Planet(°) is the elevation of Jupiter in Paris
Sun(°) is the elevation of the Sun in Paris
Moon phase is the phase of the Moon (1 = Full Moon, 0 = New Moon)

v5.21.05i Planet: Jupiter (INPOP17a)
Planet
Observatory N: 007 - Paris
Timescale: UTC
Mean equator and equinox of J2000. ICRF.

Mutual events of satellites:

Date	begin: h	m	s	end: h	m	s	Type	Dur(m)	Impact	m	Δm	limb(")	dist(")	Planet(º)	Sun(º)	Moon phase
2026	9 28	2	44 58	2	46	36	2E6	1.6	0.761	16.50	-	12.35	25.36	10.909	-28.828	0.893
2026	10 12	7	17 32	7	17	53	2E6	0.4	0.993	16.43	-	19.99	29.32	54.976	10.620	0.115
2026	10 18	4	31 3	4	33	23	1E6	2.3	0.167	16.40	-	26.60	21.65	37.996	-17.681	0.472
2026	10 28	2	52 28	3	6	57	3E6	14.5	0.327	16.35	-	12.48	40.10	27.419	-35.843	0.849
2026	10 28	4	56 21	5	9	14	3E6	12.9	0.389	16.35	-	36.81	44.62	45.965	-15.898	0.842
2026	11 6	5	25 46	5	27	47	2E6	2.0	0.538	16.30	-	4.89	38.90	52.120	-13.171	0.197
2026	11 8	2	34 49	2	39	31	4E6	4.7	0.488	16.29	-	25.41	95.41	30.450	-41.224	0.077
2026	12 3	0	20 14	0	23	36	3E6	3.4	0.837	16.13	-	40.22	55.97	23.059	-62.242	0.379
2026	12 5	0	18 56	0	22	47	1E6	3.9	0.124	16.11	-	42.09	19.28	24.090	-62.628	0.249
2026	12 19	4	6 20	4	10	15	1E6	3.9	0.400	16.02	-	43.50	17.17	54.656	-33.908	0.632
2026	12 24	4	22 42	4	25	39	1E6	3.0	0.346	16.00	-	35.48	19.26	53.536	-31.636	0.976
2027	1 22	0	34 25	0	37	53	3E6	3.5	0.413	15.87	-	2.98	27.42	53.450	-60.396	0.961
2027	1 26	20	31 14	20	32	38	1E6	1.4	0.784	15.85	-	18.80	9.56	23.595	-37.898	0.673
2027	1 28	21	57 37	21	58	31	3E6	0.9	0.985	15.85	-	35.34	17.65	38.846	-50.068	0.533
2027	2 3	3	1 8	3	2	35	1E6	1.5	0.772	15.84	-	23.57	4.65	45.685	-42.044	0.213
2027	2 11	22	20 55	22	22	58	1E6	2.0	0.040	15.84	-	1.94	1.59	50.642	-48.987	0.338
2027	2 26	2	16 51	2	18	9	1E6	1.3	0.777	15.86	-	1.15	11.02	38.168	-41.420	0.632
2027	3 6	3	13 42	3	15	53	3E6	2.2	0.899	15.88	-	28.96	30.53	23.536	-31.143	0.141
2027	3 8	19	11 48	19	14	59	1E6	3.2	0.303	15.89	-	39.70	12.83	41.073	-14.907	0.032
2027	3 22	23	5 14	23	8	45	1E6	3.5	0.169	15.96	-	39.17	17.02	50.430	-39.100	0.955

Table 4. The best eclipses of Thebe observable in France and in Europe (calculations made for Paris).

- **What is needed to observe?**

We have seen that a powerful telescope is necessary. In fact, to observe a celestial object of magnitude 14, a very large telescope is not required; a 30 cm telescope may be sufficient. For a magnitude 16 object, a 60 cm telescope is sufficient. However, in the case of Amalthea and Thebe, we recommend telescopes of 60 cm (for Amalthea) and 1 m (for Thebe) and as you will see in chapter 'Trials with a C11', now 30 cm telescopes could be successful. The presence of a bright Jupiter nearby will also necessitate a perfect sky, perfect optics, and a perfect receiver. To reduce the brightness of Jupiter, two methods are possible:

• either block Jupiter using a cleverly placed mask in front of the receiver; this is feasible but difficult and requires careful preparation (see Figure 6).

• either use a filter (see Figure 9): Methane infrared filter from 880 to 900 nm. The absorption spectrum of methane darkens Jupiter's atmosphere. In this case the received flux decreases and it is necessary either to have a larger telescope or to integrate the light with longer exposures. It seems today, according to the filter bandwidth and optical transmission, the best Methane filter is provided by ZWO (Figures 5a, 5b and 5c).

Since the goal is to precisely time a rapid transition, an extinction, or a reappearance (carefully planning the location before observing the reappearance!), desired exposures have to be around 1 s or less than 10 s, otherwise it will be impossible to time the mid-phenomenon within 0.1 s.

One advantage arises with these phenomena, which are total eclipses: therefore, precise photometry is unnecessary, as the light flux will disappear, and it is the times of the ingress then the egress we want to record. Managing offset and gain on an APS-CMOS sensor will allow us to accurately catch the sky background with the attached noise and maximise sensitivity. There are, therefore, choices to be made and several tests should be made before the observation of these satellites.

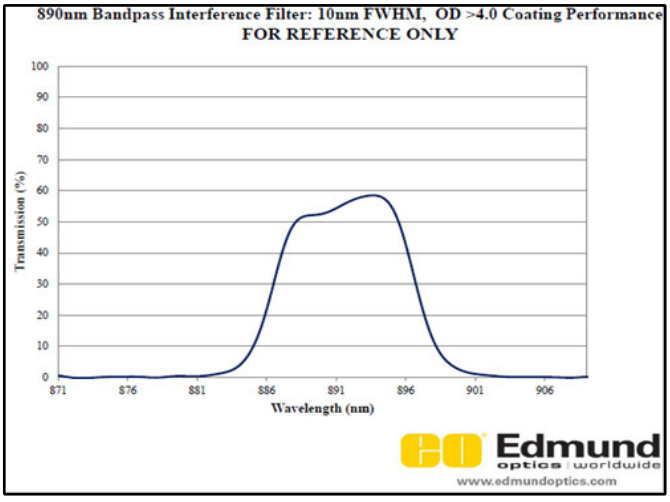

Figure 5a. Transmission curve of Methane fitted optical filter from Edmund 890 nm HBW 10 nm.

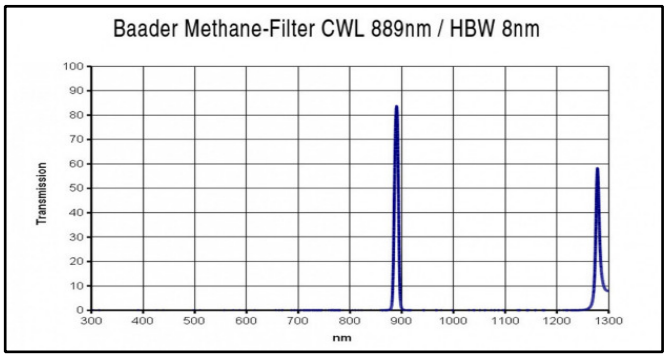

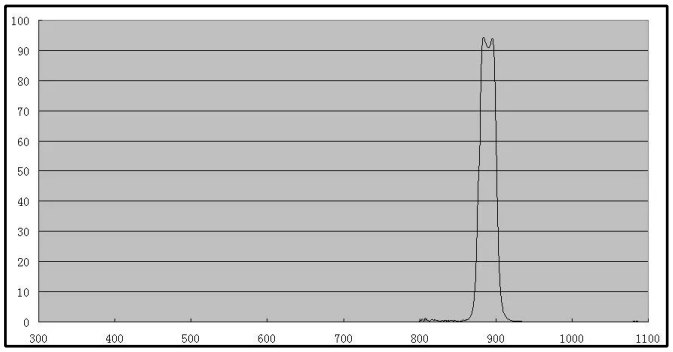

Figure 5b and 5c. Transmission curves of Methane fitted optical filters from Baader 889 nm HBW 8 nm (left) and from ZWO 20 nm FWHM (right).

Observations Made in the Past

We show here an observation of Amalthea and Thebe made with the 1 m telescope from *Pic du Midi Observatory* (OMP Observatoire Midi Pyrenees) with a mask in front of Jupiter (Figure 6).

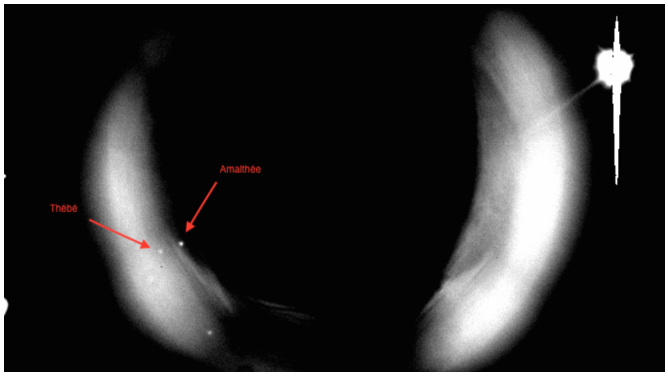

Figure 6. Amalthea and Thebe observed in visible light with a mask in front of the planet at Pic du Midi in 2015.

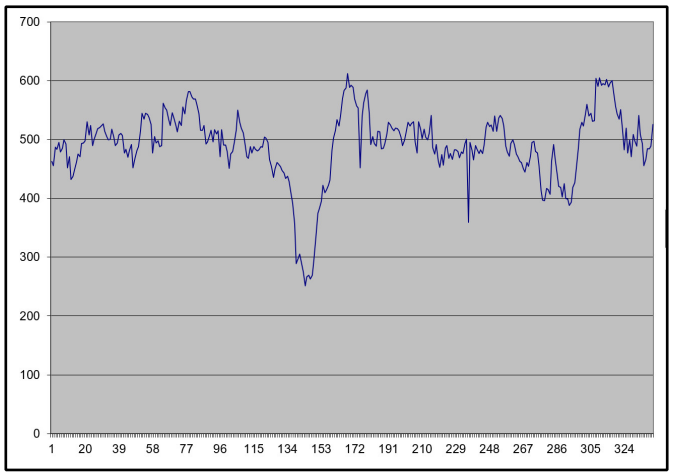

Figure 8. 2015 April 08, 20h18m00s +/-3 s UTC. Light curve of Europa eclipsing Amalthea (2E5) from 360 frames of 5 s exposure. The slipping stacking from 40 down to 5 frames along the 360 frames allows to perform a trade-off between SNR and timing accuracy. It allows to detect the eclipse from the noise and to improve the edge timing on the light curve.
(B. Christophe, A. Fernandez processing, Meudon Observatory)

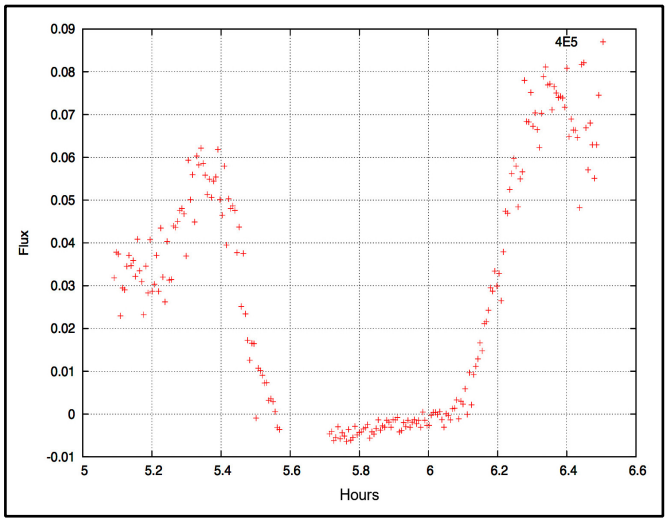

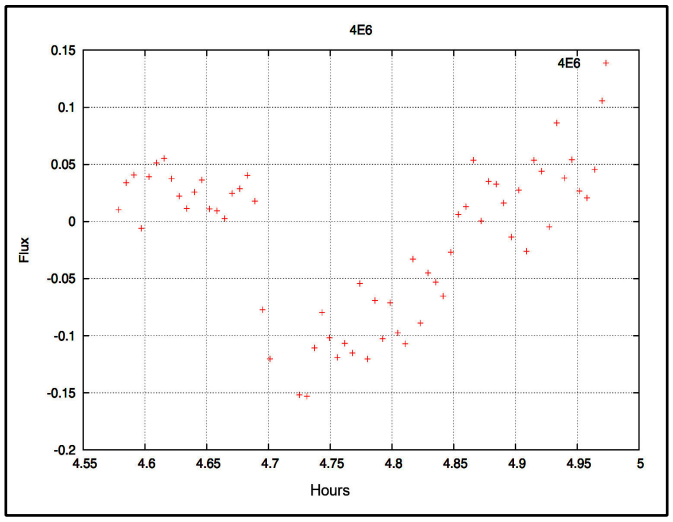

Figures 7a, 7b. Examples of light curves obtained. An eclipse of Amalthea (left) and of Thebe (right) by Callisto. (Pic du Midi with a mask on 2015 January 7)

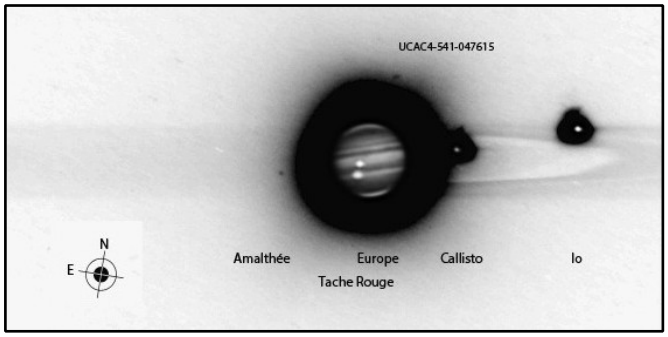

Figure 9. Stacked picture of Jupiter and Amalthea from Saint Sulpice 60 cm telescope with an Edmund 890 nm filter 10 nm (Figure 5a) in front of EMCCD Raptor camera using a 9 µm pixel pitch EMCCD gain 50%, from Texas Instruments. Stack of 360 images of 5 s exposure for Almathea and the star (20:20 UT), 360 images of 0.5 s exposure for the Galilean satellites and Jupiter (20:38 UT).
(B. Christophe, O. Dechambre, Saint Sulpice Observatory, Club Eclipse, 2015 April 08)

Trials with a C11

New APS CMOS (Active Pixel Sensor from Complementary Metal Oxyde Semiconductor fundry) cameras bring enhanced quantum efficiency in a wide spectral band, with small pixels allowing a nice sampling of the PSF (Point Spread Function) given by the telescope's native focal length and turbulence, with a less than 1e$^-$ rms read out noise in high gain mode. Thanks to the photodiode fill factor and thickness improvements new generation of Starvis Sony sensors brings this enhancement. Figure 10 shows the Quantum Efficiency from 400 nm up to 1000 nm of IMX462 Sony focal plane array. It is a full HD 1936 × 1096 array, with 2.9 µm pixel pitch and 0.5e rms read out noise in high gain mode. You may notice the 40% QE at 890 nm or more than 80% in the complete Visible band.

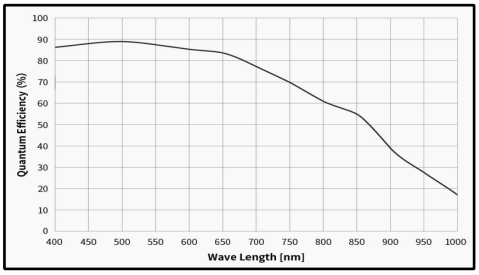

Figure 10. Quantum efficiency from latest SONY Starvis APS CMOS arrays IMX462.

Similar is the IMX585 providing a larger array. In using *SharpCap* you may accurately tune the exposure, the offset and the gain on the camera through several iterations, allowing you to put the image dynamic you need to record in the digital dynamic of the array to get both the sky background and the signal from the satellite you are looking for with the maximum sensitivity. Getting one Galilean, or better a nearby star, could be useful to track the field of view and perform frame stacking to enhance the SNR.

In addition, *SharpCap* allows you to have a smart and accurate frame time-stamping either coming from a GPS receiver like the TimeBox II or from Meinberg NTP if you are connected to Ethernet to drive the clocking of your PC.

This year M. Irzyk performed tests with a coronagraph-like sub-assembly on a C11 in order to reduce stray light. In the telescope focal plane aperture is integrated a wire with a diameter fitted to the Jupiter disk size. Then, a lens conjugates the telescope focal plane to the CMOS array. This is provided by a 25 mm macrolens in 1:1 ratio. A simple setup has been tested (during the full Moon period) in order to evaluate the efficiency of the occultation of Jupiter with a mask with the objective to increase the detectivity of Amalthea and improve SNR during Phemu events.

The setup (Figure 11) is using:

- a filter wheel (for selection Clear, Red, CH_4, … band)
- a 3D printed part
- a wire placed at the telescope focal point. The wire diameter is fitted to Jupiter's disk size.
- a 25 mm focal length macro 1:1 lens
- a CMOS camera using IMX 585

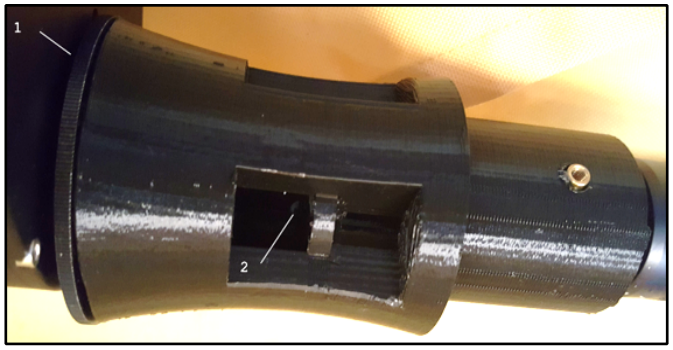

Figure 11. A specific 3D printing part has been used, linked to the filter wheel (location 1). The focus is achieved on a wire (placed in location (2). A 25 mm focal length macro lens reimages the wire in 1:1 geometry, (and so the focal plane) to the camera.

The lens is reimaging the wire (and so the telescope focal plane) on the camera. The wire has been selected to be slightly larger than Jupiter at the focus point. As a result, Jupiter is fully hidden, and only a part of the stray diffuse light is observed (Figure 12).

(Note: An autoguider would have improved the efficiency of the occultation, but was not available at the time of the test.)

The use of a relay lens with an occulting mask, slightly reduces the stray light around Jupiter and increases the SNR for the photometry measurement. It demonstrates that a 280 mm aperture with a modern CMOS camera can perform Amalthea detection. In addition, some stars in the field of view can be detected in the range of Amalthea's magnitude (Figure 13).

The 2026-2027 Phemu Campaign

The 2026 – 2027 Phemu campaign has started thanks to the first light curves released on the 2026 May 15 from Victor Bao, New Zealand and from France by J.-F. Coliac from Marseille (Figure 14). These events are easy to record, it is a nice way to start to work in the field of occultations even with small telescopes. These time-stamped recordings are less important now to improve the Galilean satellites ephemerides. However, accurate photometric light curves are interesting to probe the albedo of each satellite. Through a deconvolution process on the light curves, thanks to an accurate geometry built on accurate ephemerides, we may provide a map of the albedo distribution on the satellites. It could be done during the opposition period in a retroreflexion geometry and in the other periods with an aspect angle between the Sun illumination and from the Earth line of sight. Previous Phemu campaigns displayed some albedo discrepancies still to be understood.

Conclusion

The 2026-2027 Phemu campaign is now open! Beyond the occultations and eclipses between the Galilean satellites, we are inviting the amateur community to chase the eclipses of the inner satellites Amalthea and Thebe. These observations are difficult, and satellite observations must be practiced before the occurrence of events to determine the feasibility and the best technique. The latest APS CMOS cameras bring improved sensitivity while reducing the pixel pitch allowing amateur telescopes from 60 cm down to 30 cm diameter to try to record such light curves. Observations are encouraged because they will be useful for improving dynamical models of these satellites and thus our understanding of the Jovian system and if we may detect tides on Jupiter. The improvement of the ephemeris of Almathea and Thebe will allow the *Juice* Mission to capture images of these targets during flyby.

For more information
and for sending the observations:

phemu.imcce@obspm.fr

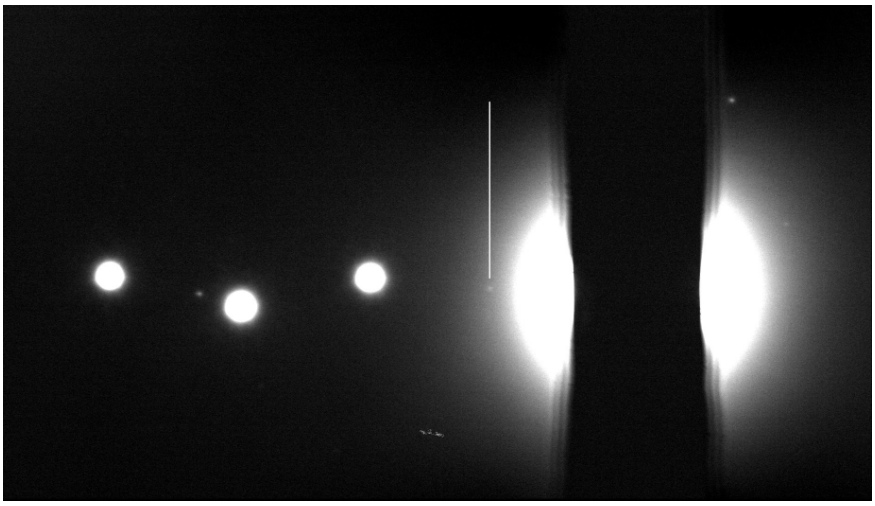

Figure 12. Stacked image of multiple short (140 × 0.5 s) exposure without any filter (Clear window). As no auto-guiding was used, the small variation of position of the mask produced the unsharp mask edge. Amalthea is clearly detected on the left of Jupiter. Figure 13 shows the identification of the detected targets.

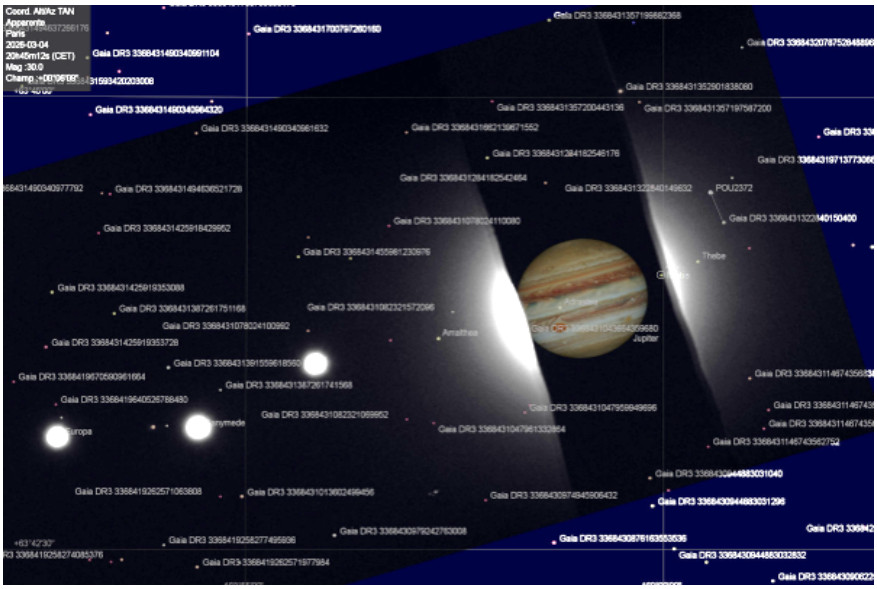

Figure 13. Due to the magnitude of Amalthea, cartography software (here Stellarium) is used to confirm Amalthea's position so as not to confuse it with nearby stars.

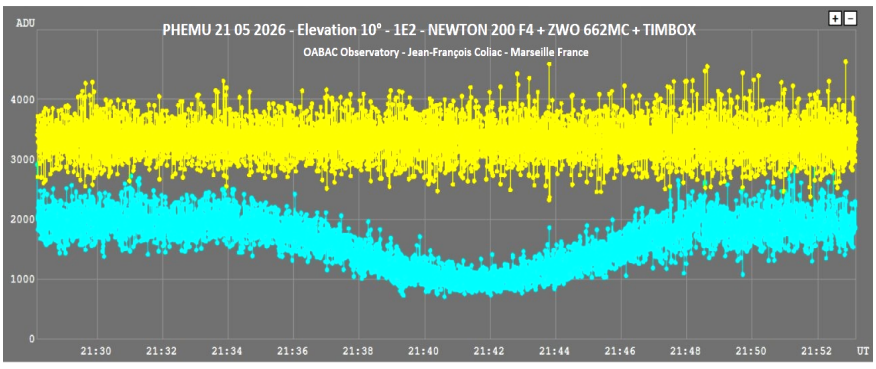

Figure 14. Phemu recorded on 2026 May 21 by J.-F. Coliac. Signal-minus-background, normalised, binning of 32 frames.

References

[1] Robert, V., Saquet, E., Colas, F., and Arlot, J.-E., CCD astrometric observations of Amalthea and Thebe in the Gaia era, Monthly Notices of the Royal Astronomical Society, vol. 467, no. 1, pp. 694–698, 2017. https://doi.org/10.1093/mnras/stx123

[2] Arlot, J.-E., Desmars, J., Lainey, V., Robert, V., The astrometry of the natural planetary satellites applied to their dynamics before and after Gaia, Planetary and Space Science, Volume 73, Issue 1, 2012, pp. 66-69, https://doi.org/10.1016/j.pss.2012.10.002

[3] Christou, A. A., Lewis, F., Roche, P., Hidas, M. G., and Brown, T. M., Observational detection of eclipses of J5 Amalthea by the Galilean satellites, Astronomy and Astrophysics, vol. 522, Art. no. A6, EDP, 2010. https://doi.org/10.1051/0004-6361/201014822

[4] Saquet, E., Emelyanov, N., Colas, F., Arlot, J.-E., Robert, V., Christophe, B., Dechambre, O., Eclipses of the inner satellites of Jupiter observed in 2015, Astronomy and Astrophysics, vol. 591, Art. no. A42, EDP, 2016. https://doi.org/10.1051/0004-6361/201628246

[9] Spectra of Planets, Spettrometria, Observatorio Astronomica "G.V. Schiaparelli", https://www.astrogeo.va.it/astronom/spettri/pianetien.htm

[10] Mohler, M., Bühl, J., Doherty, S. et al. Opening a new window to other worlds with spectropolarimetry. *Exp Astron* 28, pp. 101–135, (2010). https://doi.org/10.1007/s10686-010-9193-2

Articles and Web Links on Previous Phemu and PheSat

[5] Arlot J.-E., Emelyanov N., The Campaign of Observation of Mutual Occultations and Eclipses of the Galilean Satellites of Jupiter in 2021. Journal for Occultation Astronomy, Vol. 10, No. 4, pp. 3-10, https://iota-es.de/JOA/JOA2020_4.pdf

[6] Campagne Phému 2021 Gemini Workshop proceedings (in French), https://gemini.obspm.fr/20210101-phemus-2021/

[7] Campagne PheSat 2024 Gemini Workshop proceedings (in French), https://gemini.obspm.fr/20240215-phesat/

[8] Observational campaign of the mutual phenomena of Saturn's and Jupiter's satellites, IMCCE web page, https://www.imcce.fr/recherche/campagnes-observations/phemus/phemu

Links to Prepare the Upcoming Campaign

[11] Inner satellites eclipses dependng on the observing sites: https://www.sai.msu.ru/neb/nss/html/multisat/nsszph519he.htm

[12] Formulaires de calcul des éphémérides SEOP: https://ssp.imcce.fr/forms/satellites-events

[13] Natural Satellites Ephemeride Server MULTI-SAT: https://www.sai.msu.ru/neb/nss/html/multisat/nsszph5he.htm

[14] Configuration of the Jovian system at any date: https://www.sai.msu.ru/neb/nss/html/multisat/nssima5he.htm

[15] The site »Phemu26« providing information on the observations of mutual phenomena: https://www.imcce.fr/recherche/campagnes-observations/phemus/phemu#1

[16] The site »Pro-Am Gemini« to link observers during the Phemu26-27 campaign: https://gemini.obspm.fr/20260613-phemus-2026-2027/

Journal for Occultation Astronomy

CALL FOR OBSERVATIONS:

Impact of the 2026 August 12 Solar Eclipse on Twilight in the Mediterranean Region and other Parts of Europe

Mariusz Krukar · PTMA[1] · Rzeszów · Poland · Mariusz.krukar@gmail.com
(1) Polish Society of Amateur Astronomers

ABSTRACT: The total solar eclipse of 2026 August 12 presents a unique observational opportunity to investigate atmospheric dynamics within the twilight zone. In certain locations, totality will occur in close proximity to sunset, resulting in partial obscuration of varying magnitudes coinciding with the onset of civil twilight. The primary scientific focus of this study is the culmination of the eclipse as it occurs during successive stages of dusk along the trajectory of the lunar umbra. Because of paucity of observations of this kind of event the principal objective of this paper is to model the anticipated atmospheric and photometric phenomena. These analyses rely primarily on simulations utilising the ShowMySky 0.6 atmospheric rendering engine within Stellarium 25.4, currently recognised as a robust tool for modelling sky luminance and outdoor radiative conditions. Furthermore, orbital perspective simulations generated via SpaceEngine 0.99 are employed to visualise the interaction between the lunar shadow and the Earth's terminator line at a macroscopic scale.

Introduction

On 2026 August 12, the European mainland will experience its first total solar eclipse of the 21st century. Unlike the last totality in 1999, this event occurs during the late afternoon and approaches sunset. Due to the eclipse configuration (Gamma 0.8978), no location in Europe will experience a magnitude below 0.80, ensuring that the Earth's atmospheric response will be significantly noticeable. The most pronounced effects are expected along the exact extension of the umbral path projection and in its immediate vicinity, where the twilight sky will be profoundly affected by the umbra. Furthermore, while the eclipse duration at the surface is relatively short — lasting approximately 1 minute and 33 seconds around sunset — the umbra's passage across the lower layers of the Earth's atmosphere is expected to last over 5 minutes.

In this context, the lower layers of the Earth's atmosphere comprise the troposphere and a portion of the stratosphere. The key altitude defining this boundary is approximately 40 km, where the horizon dip is equal to 6 degrees; therefore, at this altitude, sunset is still observed at the geometrical end of civil dusk at the surface. The optimal view of the event is expected within the early civil dusk zone, as it also encompasses the anti-twilight sky. Conversely, the estimated optical limit for observing the eclipse's impact is the end of nautical twilight, when the directly illuminated sky is no longer visible above the horizon. Because astronomical twilight includes only sunlight scattered in the atmosphere, the influence of the solar eclipse during this phase should be only marginally perceptible, effectively accelerating the progression of dusk by 5 to 8 degrees.

This unusual geometric configuration may allow local observers to investigate the extension of the F-corona [1], which is typically obscured by the twilight glow. An additional accompanying phenomenon will be the coincident maximum of the Perseid meteor shower. Finally, understanding the mechanism of the lower atmosphere's response to the eclipse within the twilight zone may prove valuable in exploring the impact of the solar eclipse on the ionosphere beyond its direct geometric limits.

Methodology – Mathematical Background of the Problem

The spatial position of the lunar shadow axis, which significantly influences the twilight zone, is determined using Besselian elements [2]. These elements constitute the fundamental basis for computing solar eclipse circumstances at any given epoch [3]. The most pronounced effect of a solar eclipse on twilight conditions —specifically when the umbra traverses the atmosphere—occurs strictly between the first and second umbral contacts (U1 and U2) during dawn, or between the third and fourth umbral contacts (U3 and U4) during dusk. The umbral radius during these intervals can be derived from the following equations [3]:

$$z = \sqrt{1 - x^2 - y^2} \quad (1)$$

$$\rho_2 = |l_2 - (z \cdot \tan f_2)| \quad (2)$$

These yield an estimated umbral radius of approximately 51.5 km between U3 and U4. Consequently, the visual presence of the shadow persists in the atmosphere even after the shadow axis has left from the Earth's surface. To precisely determine the minimum altitude of the lunar shadow axis above the surface at a specific epoch, the following simplified expression is applied [4]:

$$D = \sqrt{x^2 + \left(\frac{y}{0.997}\right)^2} \quad (3)$$

Here, the coefficient 0.997 represents a ratio between the polar and equatorial Earth radius. Because this value varies slightly for each eclipse, it can be rigorously evaluated using the following generalized equation [5]:

$$\rho = \sqrt{1 - e^2 \cos^2 d}. \quad (4)$$

For the event in question, the central eclipse terminates at 18:32:12 UTC, followed by the U4 contact at 18:34:08 UTC. Factoring in the umbral radius, the maximum perturbation of twilight illumination is expected to persist until at least 18:35:32 UTC. As the U3 contact occurs at 18:30:13 UTC, the total time of umbral egress will last 5m 19s. Beyond the direct visual manifestation of the umbra, numerous geographic locations will experience a significant attenuation of ambient illumination driven by the high magnitude of the eclipse. Along the terminator line, the minimum observable eclipse magnitude is 0.82. These illumination anomalies can be quantified by comparing them against reference values for horizontal solar illumination (measured in lux) [6] at varying negative solar altitudes, employing the following formula [7]:

$$m_1 - m_2 = -2.5 \log_{10}\left(\frac{F_1}{F_2}\right) \quad (5)$$

Visualisations of the Eclipse Effect

An optimal computational approach for rendering the optical effects of a solar eclipse within the twilight zone utilises *Stellarium* (v.1.0 or later), which integrates the ShowMySky atmospheric model [8]. Developed from the sophisticated skylight rendering algorithm [9] ShowMySky computes the physical scattering of light through a planetary atmosphere in real time. Powered by the external CalcMySky C++ library [10], the rendering engine incorporates multiple-order scattering and ozone absorption (specifically within the Chappuis band) during twilight period. Crucially, this model generates physically accurate atmospheric effects during solar eclipses by utilising a three-tiered eclipse simulation quality parameter. This yields realistic luminance attenuation and chromatic shifts across the celestial dome during lunar transits.

When coupled with a hemispherical (all-sky) projection, the ShowMySky model provides a robust framework for simulating the eclipse's impact on twilight phenomena. The software allows for simulations from arbitrary geographical coordinates, enabling the analysis of the eclipse under varying solar depression angles. The resulting rendering accurately reproduces the umbral shadow column and the emergent background stellar field, approximating human visual perception as shown in Figure 1.

Figure 1. The umbral column projected from Bizerte (37°16′ 27.92″N; 9° 52′ 26.08″ E) at 18:32:30 UTC on August 12, when the Sun will be approximately 3.5° below the horizon.

Figure 2. The anti-twilight arch truncated by the umbra projected from Galite Islands (37°31′ 30.82″N; 8° 55′ 46.63″ E) on August 12 at 18:32 UTC with comparison to the same moment a day after.

However, a notable limitation is that the simulated visual threshold for stars is achieved prematurely; the current Stellarium engine does not account for the physiological temporal kinetics of human dark adaptation (the transition to mesopic or scotopic vision) in response to sudden drops in ambient illumination [11]. The simulated eclipse dynamics exhibit notable optical phenomena in the antisolar hemisphere (the anti-twilight sky). Under standard twilight conditions, observers witness the ascent of the Earth's shadow as a dark blue band capped by the anti-twilight arch, commonly known as the Belt of Venus. Because the rendering engine relies on multiple-order scattering, the introduction of the lunar umbra accurately demonstrates the spatial interruption and truncation of the Belt of Venus, like in Figure 2.

Furthermore, the projection of the lunar shadow can be analysed from an extraterrestrial perspective using SpaceEngine (v.0.99). By employing High Dynamic Range (HDR) rendering with incremental exposure adjustments, this software simulates orbital vantage points that are largely unattainable via standard satellite imagery. This perspective is vital for visualising the complex shadow dynamics during the extreme contact phases of a total solar eclipse (e.g., between the U1–U2 and U3–U4 contacts), particularly when the umbra intersects the terminator line [12] as Figure 3 indicates for us.

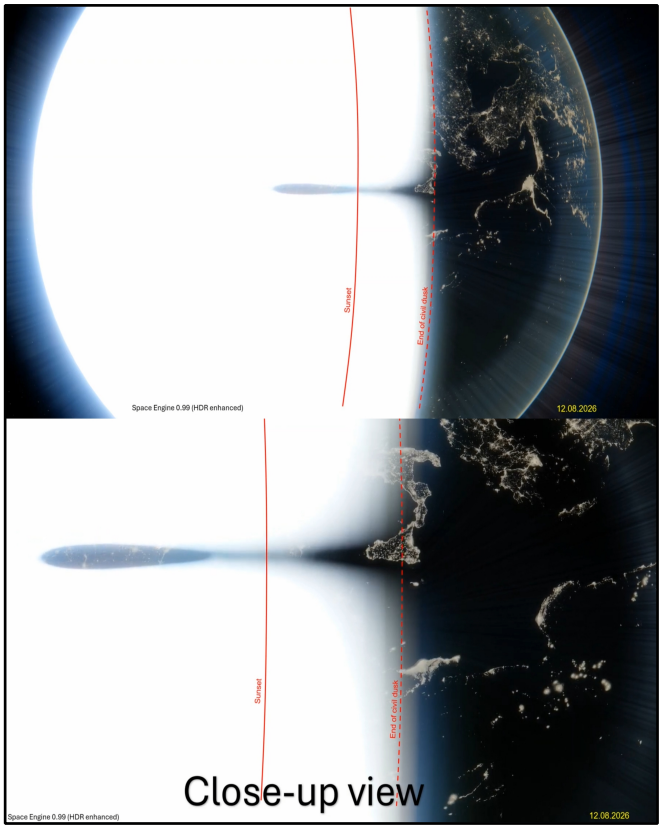

Figure 3. The projection of umbra shortly before its U3 contact from the space perspective (Space Engine 0.99)

The Twilight Disturbance Model

Calculating the differential in ambient illuminance between an unobstructed Sun and a partially-obscured Sun across various eclipse magnitudes facilitates the modelling of eclipse-induced twilight under any given circumstances.

Because a variable fraction of solar radiation is blocked, the standard progression of twilight is altered: dawn is delayed, while dusk is correspondingly advanced. These calculations allow a precise estimation of the correlation between typical and eclipse-induced twilight, demonstrating that every phase of an eclipse-altered twilight has a direct optical equivalent under standard atmospheric conditions.

By analysing specific obscuration levels, observers can quantify the deviation between normal and eclipse-induced twilight. For instance, at approximately 80% solar obscuration, the perceived twilight deepens by an equivalent of 2 degrees of solar depression. Practically, this means the ambient lighting characteristics typically associated with the end of civil twilight manifest prematurely, when the solar depression reaches only 4 degrees. A comprehensive comparison of these variables is detailed in the accompanying nomograph presented in Figure 4.

Furthermore, twilight progression can be comparatively analysed by plotting the relationship between ambient illuminance and solar depression. The occurrence of an eclipse disrupts this standard decay curve, accelerating or decelerating the twilight phases depending on the progression of the eclipse. By modelling the changing magnitude of the eclipse throughout the twilight period, it is possible to accurately predict the exact moments when specific celestial bodies and phenomena, such as the Milky Way, will become visible to the naked eye (Figure 5).

Assuming a constant obscuration magnitude across the entire twilight zone, post-civil dusk conditions occur earlier in the evening, and pre-civil dawn conditions persist later into the morning. At higher eclipse magnitudes, this atmospheric optical disturbance becomes pronounced enough to significantly alter the standard rate of illuminance decay, potentially inducing periods where ambient light levels remain temporarily static.

Discussion

The termination of a geometrical total solar eclipse does not signify the cessation of its associated atmospheric optical and astronomical effects; rather, these phenomena attenuate as a function of increasing solar depression. The most pronounced visual impacts of an eclipse occur during the early stages of civil twilight. Even in the absence of direct solar irradiance at the surface, tropospheric clouds can exhibit dynamic chromatic shifts due to high-altitude sunset illumination. Consequently, transient optical phenomena, such as shadow bands or the retreating umbral cone, may remain discernible. Given that typical commercial cruising altitudes often intersect with upper-level cloud decks,

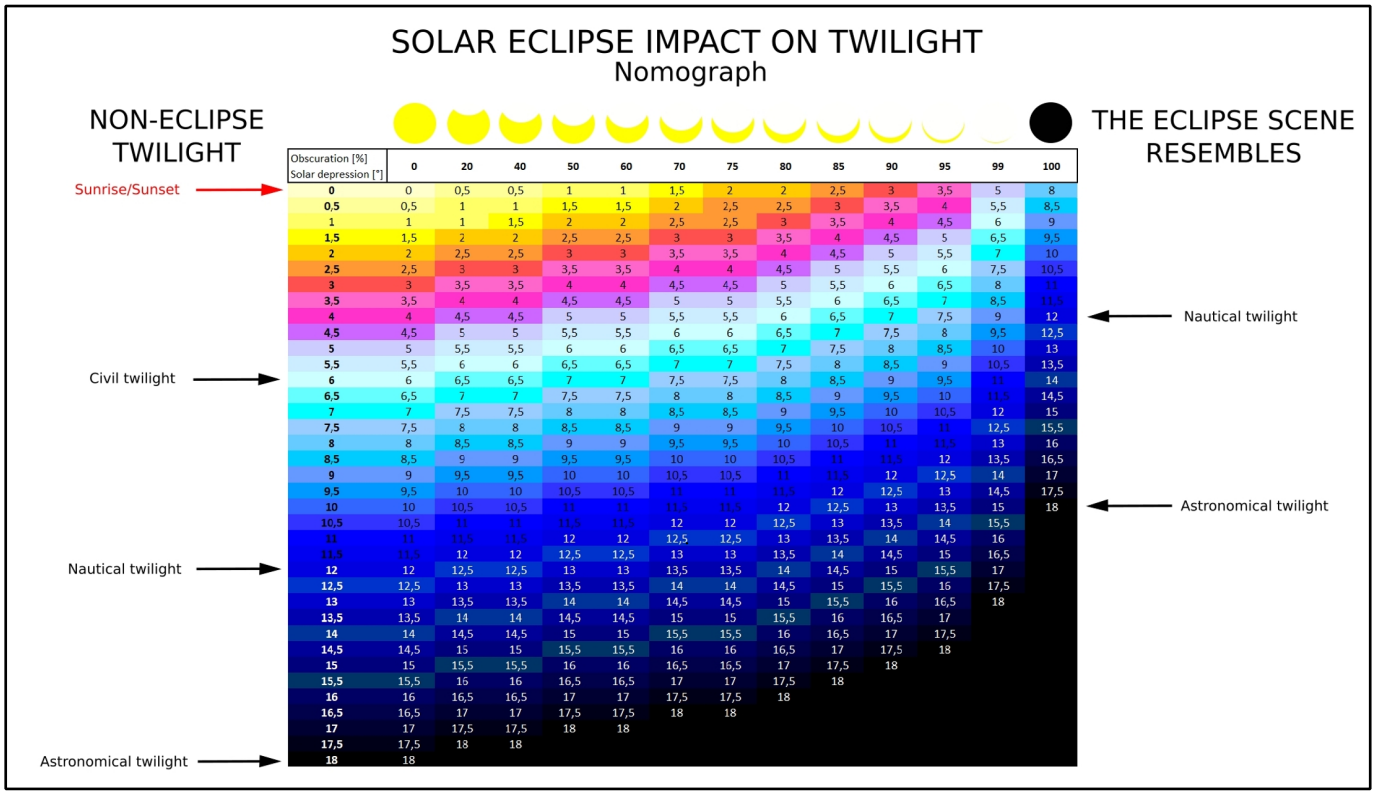

Figure 4. The solar eclipse impact on twilight nomograph.

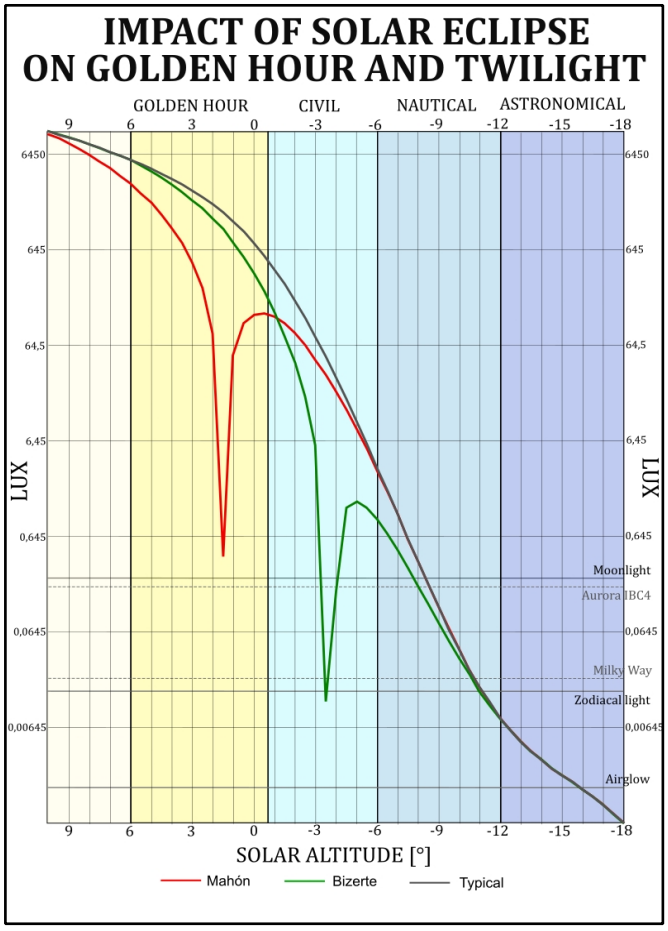

direct solar illumination can persist until the end of civil twilight under optimal atmospheric conditions. At the terminus of the eclipse path, the tangent geometry of the umbra causes it to stretch across the celestial dome (Figure 6).

Of particular interest is the anti-twilight region, which exhibits dynamic transformations at shallow solar depression angles. Beyond the geometric intersection of the umbra and the Earth's shadow — which effectively truncates the anti-twilight arch — observers can detect significant chromatic alterations induced by solar limb darkening, resulting in a pronounced red shift.

The perturbation of the anti-twilight sky by a solar eclipse is most prominent up to a solar depression of 4°, at which point the Belt of Venus attenuates and the anti-twilight arch dissipates. The solar hemisphere of the sky remains optically complex throughout the twilight continuum, exhibiting both direct and forward-scattered solar radiation. Eclipse-induced photometric anomalies in the solar azimuth remain discernible until a solar depression of 12°, marking the transition from nautical to astronomical twilight and the point at which the lower atmosphere is entirely deprived of direct insolation.

Figure 5. The impact of solar eclipse on golden hour and twilight computed for Mahón at Menorca (red), where totality will occur 1.5° above the horizon and Bizerte, where in almost the same moment the totality will have an impact on civil dusk at solar position of 3.5° below the horizon (green) with comparison to typical illumination [lux] drop in normal conditions.

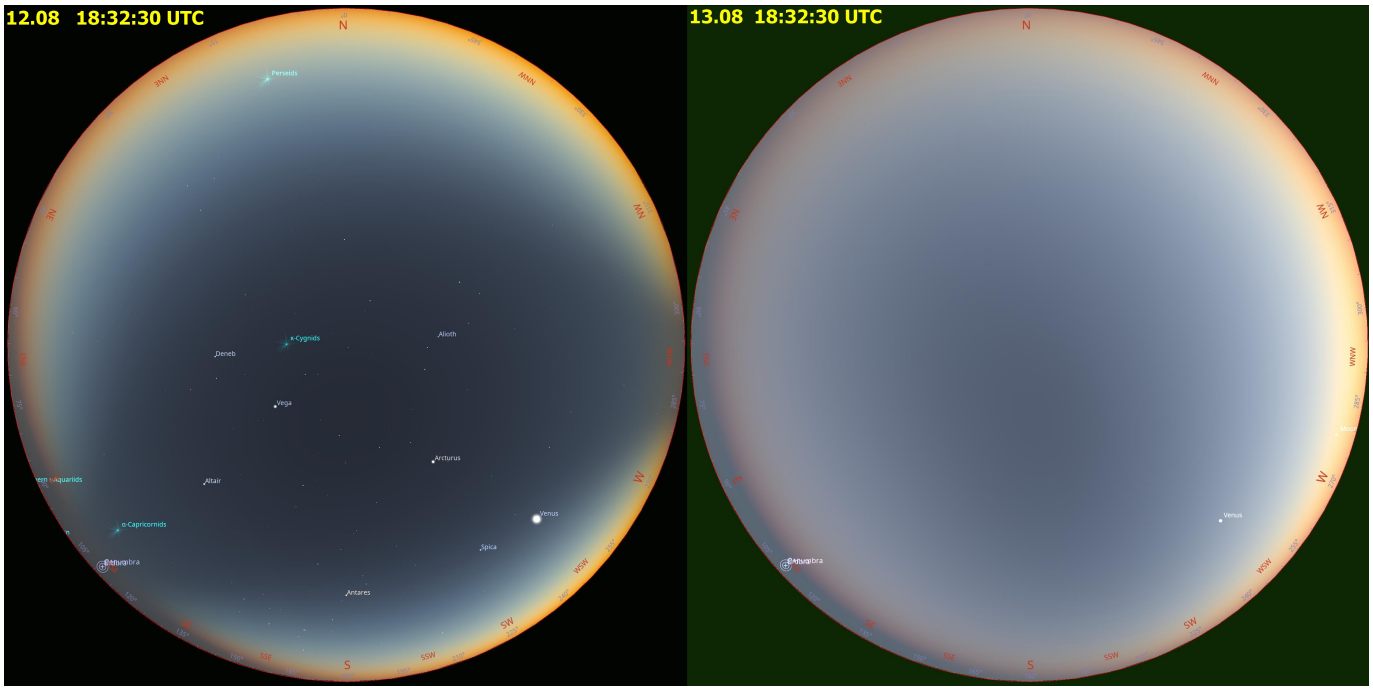

Figure 6. The projection of umbra stretching across the entire sky at solar depression of about 2° possible to see on August 12 at 18:32:30 UTC at Mediterranean (37°42' 29.08"N; 8° 11' 55.27" E) around 100 km south of Sardinian coast with the comparison of the sky view a day after at the same time.

Figure 7. The estimated view of early astronomical twilight at solar depression of approximately 13.5° from Bengazi, Libya (32°6′ 53.50″N; 20° 4′ 6.92″ E) with comparison to the same moment of twilight in non-eclipse conditions 24 hours later.

Calculating the differential in ambient illuminance between an unobstructed Sun and a partially obscured Sun across various eclipse magnitudes facilitates the modelling of eclipse-induced twilight under any given circumstances.

Furthermore, due to the absence of direct scattering in the lower troposphere — particularly within the planetary boundary layer — the umbral structure can remain visible from off-centre locations, extending tens of kilometres beyond the projected path of totality.

During astronomical twilight, variations between eclipsed and non-eclipsed baselines are probably minimal; with the umbral column no longer geometrically defined, the primary differentiator is the integrated sky surface brightness (Figure 7).

Proximity to the extended path of totality introduces a notable photometric anomaly: a non-monotonic illuminance curve characterised by distinct temporal shifts [13]. Following a rapid deceleration in ambient light levels driven by deep partial eclipse magnitudes, illumination rebounds post-maximum, creating a secondary, localised maximum. These temporal variations result in periods where ambient brightness plateaux, a phenomenon colloquially referred to as a "twilight standstill." Observers situated further from the centreline experience a singular manifestation of this effect: at eclipse maximum, the standard progression of twilight decay temporarily arrests — preceded by a period of accelerated darkening — before resuming its typical descent. For locations at minimal eclipse magnitude, the eclipse impact is essentially twofold: a rapid acceleration of darkness followed by an opposing illuminance rebound after the greatest phase is achieved (Figure 8).

Depending on the temporal alignment between maximum eclipse obscuration and local sunset, the perturbation of twilight illumination manifests in three distinct observational regimes. The first scenario, applicable to the majority of the Iberian Peninsula, occurs when totality precedes sunset; consequently, the setting of the partially or fully eclipsed solar disk directly modulates the photometrics of early civil twilight.

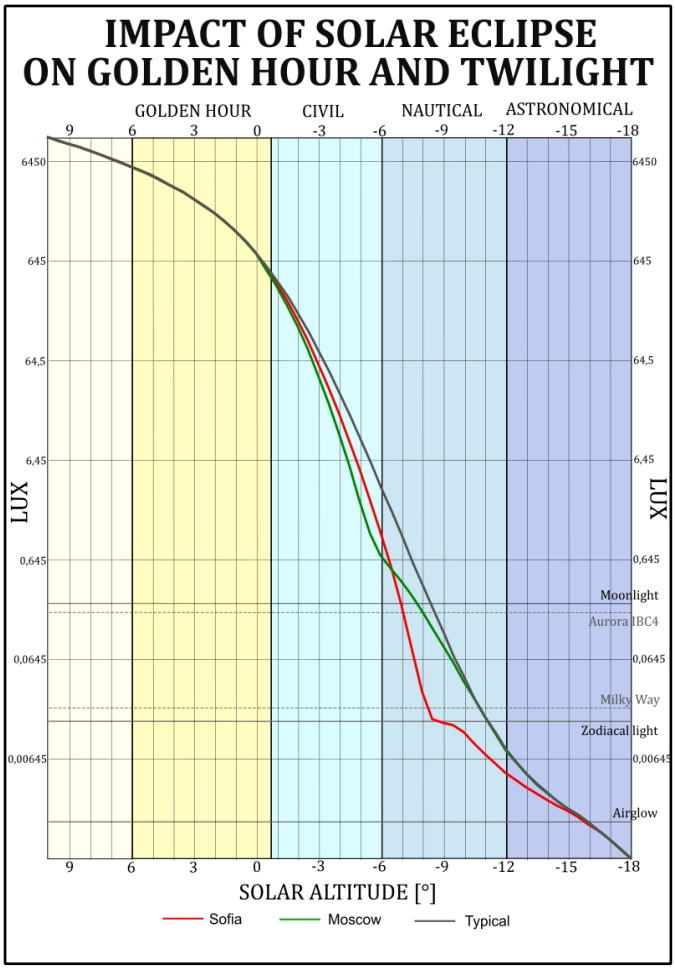

Figure 8. The influence of deep partial solar eclipse on twilight as computed for Moscow (green) and Sofia (red). In both locations the I contact occurs almost at sunset. Depending on latitude, the greatest eclipse occurs at the end of civil or mid-nautical dusk.

The second situation arises when the initial contact phases occur before sunset, resulting in maximum obscuration precisely coinciding with the Sun's geometric descent below the horizon. Finally, a third regime characterises locations where the eclipse is geometrically unobservable due to the solar disk remaining entirely below the horizon; nevertheless, the event induces measurable anomalies in twilight sky brightness via high-altitude atmospheric scattering or even direct shadow column visibility.

How to Observe

Proper alignment of the observational axis is the most critical parameter in this methodology, requiring precise determination of the viewing azimuth. Along the exact path extension, the viewing geometry is straightforward, necessitating observations strictly along the solar and anti-solar vectors. For observation sites situated outside the primary path extension, predictive modelling using computational planetarium software, such as *Stellarium*, is recommended to simulate the optical phenomena prior to field deployment.

Observing the culmination of the eclipse's impact on twilight is most effectively achieved by monitoring the solar sector of the sky, which exhibits peak luminance following sunset. Even under total solar eclipse conditions, direct sky illumination remains sufficient for detection by consumer-grade optical sensors, including mobile device cameras. However, during nautical twilight, high-sensitivity digital single-lens reflex (DSLR) astrophotography techniques are typically required. Conversely, monitoring the anti-solar twilight sky necessitates long-exposure photography under all scenarios due to the inherently low photon flux in that region. The choice of optical instrumentation is equally critical; capturing the full spatial extent of the phenomena requires wide-angle lenses, preferably with focal lengths of 18 mm or shorter. Within the early civil twilight zone, where the anti-solar sky presents significant optical variations, the deployment of all-sky lenses is highly advantageous. Documenting the event during astronomical twilight remains the most technically demanding phase, strictly requiring prolonged exposure intervals to capture an adequate optical signal.

Visual and photographic documentation of the event constitutes a vital component of the observational campaign. To accurately isolate and quantify minor fluctuations in illumination and spectral banding, this methodology requires a comparative analysis against control observations. These baseline measurements must be conducted during identical twilight phases outside of eclipse conditions [14]. Provided atmospheric conditions are sufficiently transparent [15], these variations typically become perceptible even at low magnitudes of solar obscuration. In addition to visual documentation, the continuous recording of sky brightness disturbances provides crucial quantitative data. This metric can be systematically monitored using automated sky quality meters, such as the Unihedron SQM-LU-DL, which interface directly with local or remote computing systems [16]. By configuring specific, high-frequency logging intervals, researchers can acquire high-resolution datasets of localised sky surface brightness, measured directionally in magnitudes per square arcsecond (mag/arcsec^2) [17]. These values can subsequently be converted to standard photometric units (lux) for broader comparative analysis. Furthermore, ambient illuminance can be precisely quantified using Class A photometric sensors equipped with continuous data-logging capabilities. Instruments such as the LXP-10A luxmeter [18] are optimal for this application, offering a detection threshold capable of resolving illuminance differentials as minor as 0.001 lux. Finally, chromatic shifts in the sky induced by the eclipse can be recorded using DSLR or mirrorless camera systems. To ensure photometric integrity and retain maximal spectral data, it is imperative to capture images in a minimally processed (RAW) format. Moreover, all exposure parameters must be manually locked; in particular, establishing a fixed white balance is essential to objectively capture true chromatic shifts without the interference of internal algorithmic auto-correction.

Conclusions

The 2026 August 12 total solar eclipse presents an unprecedented opportunity to investigate atmospheric dynamics beyond its direct geometric path. As the umbral trajectory terminates east of the Balearic Islands, it will significantly perturb twilight conditions across the central Mediterranean region, transiently encompassing the celestial dome. This photometric anomaly facilitates comprehensive, multi-perspective documentation of atmospheric scattering and irradiance throughout the twilight continuum.

The author will be very pleased to perform any analyses, as the topic itself is pioneering in modern times. Despite several publications, there is an utter lack of visual reports of events such as this. All the results will be collected under [19].

References

[1] Gulyaev, R. A., On a possible use of total solar eclipse below the horizon for observations of the inner zodiacal light (as applied to the eclipse of 30 June, 1992), Laboratory of Solar Activity, IZMIRAN, [Pushkov Institute of Terrestrial Magnetism, Ionosphere and Radio Wave Propagation Russian Academy of Sciences], USSR Academy of Science (1992), Solar Physics 137, 209-211, 1992, https://ui.adsabs.harvard.edu/scan/manifest/1992SoPh..138..209G

[2] Espenak, F., Besselian elements for the total solar eclipse of August 12, 2026; Eclipse Predictions by Fred Espenak, NASA's GSFC (2025-09-07), https://eclipse.gsfc.nasa.gov/SEbeselm/SEbeselm2001/SE2026Aug12Tbeselm.html

[3] Meeus, J., Elements of solar eclipses 1951-2200, Willmann-Bell Inc (1989)

[4] Deakin, R. E. and Hunter, M. N., Geometric Geodesy part A, School of Mathematical and Geospatial Sciences, RMIT University [Royal Melbourne Institute of Technology], January 2010, pages 151 https://www.mygeodesy.id.au/documents/Geometric%20Geodesy%20A(2013).pdf

[5] Meeus, J., Astronomical algorithms – 2nd edition, Willimann-Bell Inc (1998)
[6] Schlyter, P., How bright are natural light sources?, (2023), https://stjarnhimlen.se/comp/radfaq.html#11
[7] Meeus, J., Astronomical formulae for calculators, 3rd edition, Willmann-Bell Inc (1982)
[8] Zotti, G., Wolf, A., Stellarium 26.1 User Guide (2026), https://stellarium.org/files/guide.pdf
(9] Bruneton, E., Neyret, F., Precomputed Atmospheric Scattering, Proceedings of the 19th Eurographics Symposium on Rendering 2008, vol. 27, Computer Graphics Forum 4 Eurographics, Wiley, p.1079-1086
[10] Anonymous, CalcMySky v0.3.1 using in Stellarium, (2025-02-09), https://10110111.github.io/CalcMySky/using-in-stellarium.html
[11] Anonymous (Atque), Github.com: Objects visible too early in twilight #4291, (2024-09-07), https://github.com/Stellarium/stellarium/issues/4291
[12] Krukar, M., A strange effect at solar eclipses below the horizon; (2026-01-24), https://astro-geo-gis.com/a-strange-effect-at-solar-eclipses-below-the-horizon/
[13] Geyer, E. H., Hoffmann, M., Volland, H., Influence of a solar eclipse on twilight, Appl. Opt. vol. 33 (issue 21), pages 4614-4619 (1994), Optica Publishing Group, Washington D.C., https://doi.org/10.1364/AO.33.004614
[14] Krukar, M., Solar eclipse below the horizon – the observation guide (2023-11-23); https://astro-geo-gis.com/solar-eclipse-below-the-horizon-the-observation-guideline/
[15] Dearborn, D., Lynch D.K., Richtsmeier S.C., Antitwilight II: Monte Carlo simulations, Applied Optics, Jul 1, vol. 56 (issue 19), pages G169-G178 (2017)
[16] Anonymous, Sky Quality Meter – LU- DL (2025-09-19); https://www.unihedron.com/projects/sqm-lu-dl/
[17] Krukar, M., Great American Eclipse visible from Europe (2025-09-25); https://astro-geo-gis.com/great-american-eclipse-visible-from-europe/
[18] Anonymous, Sonel LXP-2, LXP-10B, LXP-10A light meters (2023-10-02); https://2jl.com.pt/wp-content/uploads/2017/04/Luximetro.pdf
[19] European Eclipse Quadruplet, 2026 TSE, https://eeq.astro-geo-gis.com/tse-2026/

Journal for Occultation Astronomy

You Think You Might Have Discovered an Asteroidal Satellite? Special Reporting Requirements

Dave Herald · TTOA · Murrumbateman · Australia · D.Herald@bigpond.com
Dave Gault · TTOA · Hawkesbury Heights · Australia · djgault57@gmail.com
Jean-François Gout · IOTA · Starkville, Miss. · USA · jfgout@gmail.com
Kazuhisa Miyashita · IOTA/EA · Azumino, Nagano · Japan · k_miyash@nifty.com
Christian Weber · IOTA/ES · Berlin · Germany · christian.weber@iota-es.com

ABSTRACT: The assessment of an observation to establish whether or not it involves a satellite, and the subsequent drafting of a CBET, involves some routine data items and measurements. It is helpful if the observer provides all this data available at the start of the process.

General Requirements for Satellite Determination

- Exclude peripheral explanations. Measurement tracking errors, birds, planes etc.

- Exclude a double star explanation. Generally, both drops should be to the same depth, with that drop being at least 1.0 mag. However, if the diameter of the satellite (or even the asteroid) is small, Fresnel diffraction may result in different light drops – in which case the sum of the drops must be greater than the drop if the star was a single star before consideration of Fresnel diffraction is entered into.

- Importantly, this means that the exposure used for recording the event must be sufficient to include stars 1.0 mag fainter than the target star. If the recording does not include comparison stars that are at least 1.0 mag fainter than the target, a double star explanation for the light curve cannot be excluded.

- Exclude a graze as an explanation. If the interval between the start of the first drop and the end of the 2nd drop is less than the maximum event duration, the event will most likely be a graze. Larger differences may or may not be explained by a graze – an issue that is dealt with in the detailed analysis, which will consider the effects of shape models and possible body elongations implied by rotational light curve variations. Previous occultations by the asteroid may also be reviewed.

What You Should Provide

When measuring the recording:

- Stars of similar brightness to, or brighter than, the target star are only useful for tracking during the measurement, and (if needed) for normalising the light curve for noise variations. For assessing a satellite, the essential requirement is for faint comparison stars.

- Include at least one comparison star that is at least 1.0 mag fainter than the target star. Preferably more than one. The absence of any such a star in a recording will likely prevent a positive determination of a satellite.

- Highly desirable (required unless there are no stars to meet this requirement). The comparison stars should have the same 'colour temperature' as the target star. To do this, you need to compare the difference between the visual and red magnitudes of the target star against that difference for the comparison stars. The value V-R of the faint star should be similar to the V-R of the target star. Differences of up to around 0.4 are okay. Larger differences may be a problem, in which case you should find a different star (if you can).

- Make a visual inspection of the sequence of frames in the two light drop regions to confirm each light drop is 'real' and not the result of a measurement tracking error. Expressly include in your report the result of the check.

- Save the .csv file of the measurement from that software. If you have created a VizieR light curve file, include that as well.

When reporting the measurement:

- If you are using *Tangra* [1], include a copy of the .lc file. If you know how to use *Tangra*, but don't usually use it, make an additional light curve measurement with Tangra, and include the .lc file.

- The star number identifier of all stars used.
  For the plot showing the light curves for the target and comparison stars, clearly relate each comparison star to its light curve.

- An estimate of the limiting magnitude of the recording.
  That is, the magnitude of the faintest stars that are reliably present in the great majority of images in the recording. Provide the limiting magnitude in both Visual and Red. You should make the limiting magnitude assessment on the same basis as when you measure the recording. That is, if you measure every frame of the recording, the limiting magnitude must also be made on the basis of individual frames. Assessing the limiting magnitude by stacking multiple frames to improve the signal to noise is unacceptable.

- The usual reporting details of the event, with a report for each D+R sequence.
  This may be two spreadsheet .xls files for North America and Australasia, or (for Europe) two reports in SODIS [2]. Desirably an *Occult* '.xml' file created by your regional team. At the very least: date and event times, star number, asteroid number, site coordinates. Plus a copy of the light curve image as generated by your usual measurement software.

- Your name and affiliation, like:

  - 'C. McPartlin, International Occultation Timing Association (IOTA)'

  - Your observing location and equipment (including the basis of the time source). Some examples are:

    - observed from Goleta, CA, USA using a 13-cm telescope with an Astrid GPS-disciplined CMOS video system.

    - observed from Starkville, MS, USA using a 28-cm telescope, a CMOS camera, and a Linux computer synchronised by Network Time Protocol (in which the accuracy of his time synchronisation has been tested multiple times with a GPS-triggered flasher and found it to be always better than 10 ms)

    - observation was made near Stevenage, Hertfordshire, UK, using a 35-cm telescope (+ ASI432 CMOS camera)

    - observation was done at Charlottesville, VA, USA, using a 28-cm telescope (+ QHY5III-200MM camera with GPS-linked timing)

- Be prepared to make your event recording available if requested – in case the assessment process considers it appropriate/desirable to re-measure the recording, including using a different measurement tool.

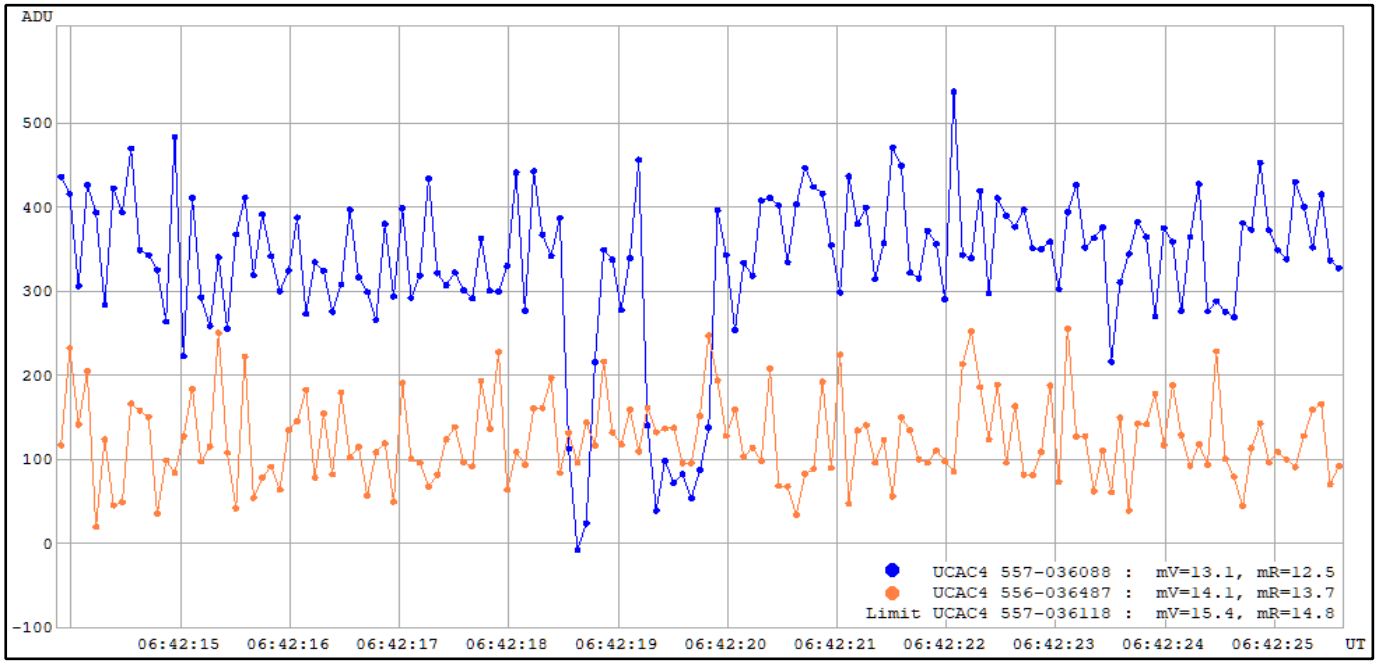

Figure 1. Example of a well presented light curve image. It identifies the measures of the target and comparison star, as well as the star catalogue identifier, and V and R measures.

Getting Magnitudes and Star Identifier

In principle, there are various ways of doing this – such as by matching stars in the C2A star chart to your images.

However, there is a much easier way of undertaking this task - use the star chart functionality in *Occult* [3]. In doing this, you should make sure you have installed the Gaia16 star catalogue, so that the map includes all stars to magnitude 16.0.

The critical functionality provided in the *Occult* star chart is that you can make the star chart transparent (Figure 4). This enables you to:

- place the *Occult* star chart over an image from your recording. With the chart drawn as black stars on a white background, you will be able to see both the stars on the star chart, and the stars on your recording

- match the scale and orientation of the chart to match your recording. The chart can be rotated a full 360°, flipped horizontally and/or vertically, and the scale varied to match your image size.

Main Menu Items for Matching the Star Chart to Your Image

The easiest way to undertake this process is via *Occult Watcher* [4]. Open the event in *Occult* with a right-click on the relevant event line. [If you haven't done so, you will need to add the *Occult* addin into OW, using the add-ins menu item in OW]. At the top of the *Occult* plot there is this icon (Figure 2).

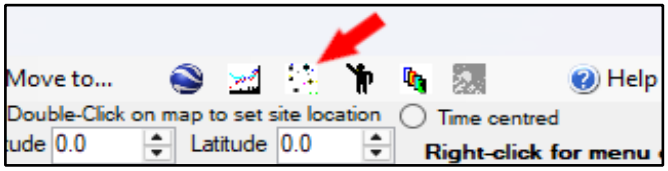

Figure 2. Icon to open the menu for star chart overlay in Occult.

Click it to open the star chart. The chart will be centred on the target star (which is circled), with marks indicating the motion of the asteroid at hourly intervals.

The first time it is used you will need to set the map size and orientation. This is done using the Menu items Size..., Magnitude... and those listed under 'with Plot....' menu item. Once you have made these settings, you can retain them for whenever the chart is opened, using the menu item 'with Plot... Store current settings' (Figure 3).

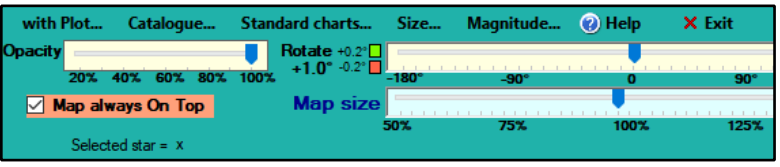

Figure 3. Plot setting menu for star chart overlay in Occult.

The chart form is made transparent using the slider at top left. The check box **Map always On Top** is to make sure the form doesn't accidentally get covered by other forms.

This arrangement allows you to directly match stars on the star chart to stars in your recording – including stars which are barely visible in the recording (Figure 4). It also allows you to identify stars that are not visible in the recording – which is very relevant to establishing the limiting magnitude of the recording.

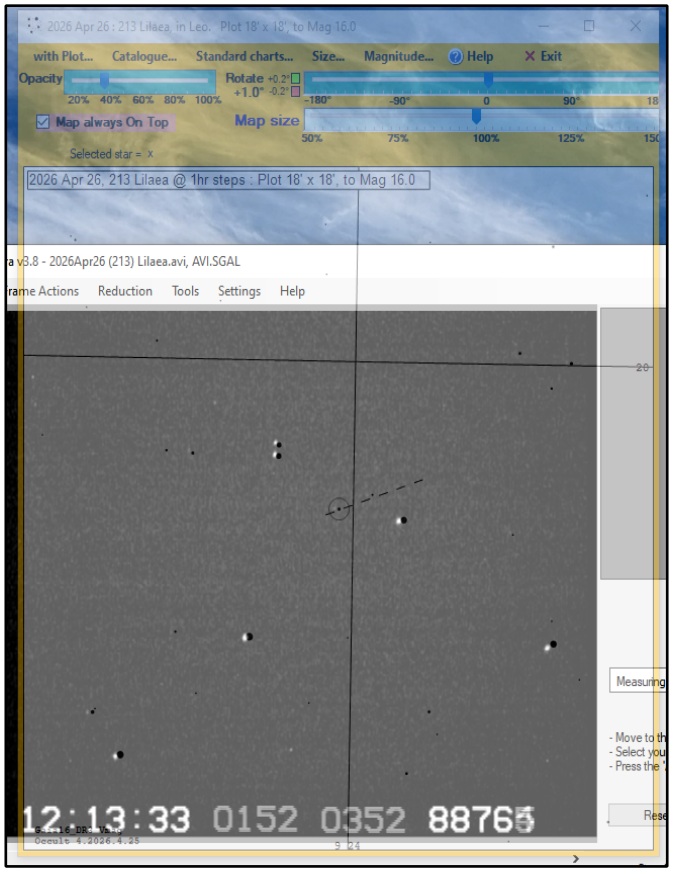

Figure 4. Example of chart over an image.

To get the details of any star on the star chart, simply place the cursor on it, and click. The details of that star will appear just above the plot area, as in Figure 5. This gives you the star identifier, the V magnitude, the colour values of B-V and V-R, and coordinates.

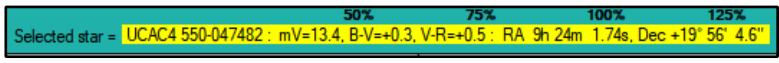

Figure 5. Star details after clicking on a star on the map.

You can keep a list of stars you are measuring this way. On the menu item click **with Plot... Record and copy details of selected stars**. This will open a box, as in Figure 6. Simply click the Add button to add the displayed details of your selected stars. You can locate any star in the list by clicking on the star entry – which will result in the relevant star being highlighted with a small purple square.

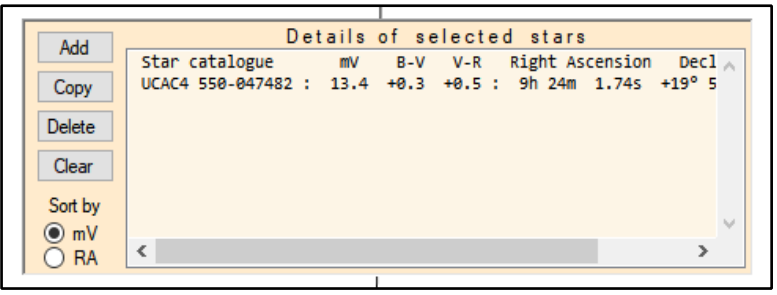

Figure 6. Table of details of selected stars.

The stars can be sorted by V magnitude (for assessing the limiting magnitudes) or by RA (for ease of identification on the plot). The process is very quick and reliable. Once the chart is matched to your image, you can select the required stars (with all their details) within a very small number of minutes – without any manual matching to other sources (Figure 7).

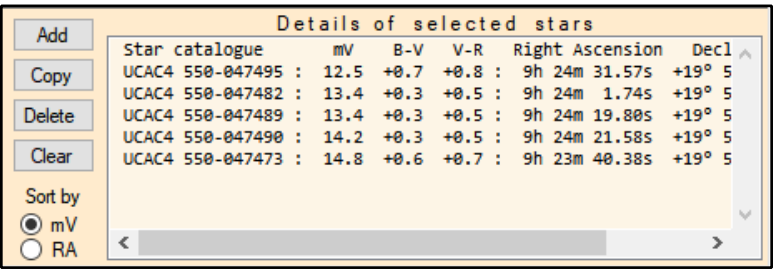

Figure 7. The target star is the 3rd in this list. The 4th star is just visible. The 5th is not visible. As a result, the limiting magnitude would be assessed as 'about' 14.2 V, 13.7 R. [The R magnitude is derived as mV - (V-R)]

The colour temperature of these stars is assessed using the V-R and/or the B-V values. Desirably, the V-R and B-V values for the comparison stars should be similar to those of the target star. In Figure 7, the target star is the 3rd star. The V-R and B-V values for the 2nd and 4th stars are the same as the target star, making them ideal comparison stars. The values for the 1st and 5th stars are a little different but are still close enough to be used reliably. If the difference is greater than around 0.4, you should try to find other stars that have a better match. If the differences are much over 0.5 (in one or both), the star is probably unsuitable as a comparison star and should only be used in desperation.

Copy this list and include it with your report – indicating which stars in the list (if any) are not visible.

Why Do We Have to Consider Both the V and R Magnitudes?

We are making white-light recordings of the event, with cameras that have a sensitivity that is dependent on colour. To avoid any issues associated with the camera response for different colours, we aim for the comparison stars having the same colour as the target star. That way we can confidently assert that the light level of the comparison star is directly comparable to the target star – irrespective of the camera response. This is a very important issue when asserting a light drop from the target star to the comparison star does not have a component due to a different camera response to different colours; that any difference in brightness is a 'real' difference and not a colour-affected camera-response difference. In particular, the measurement of the magnitude drop needs to be made in both colours.

What Happens with My Observation?

The objective of a claim to a satellite discovery is the formal recognition of it by the International Astronomical Union (IAU) by way of publication in a Central Bureau Electronic Telegram (CBET) [5]. This is a serious issue. It is not the same as sharing your observation with your friends, local astronomy club or IOTA. Rather it is the making of a claim in the formal environment of professional astronomers, with that claim needing to be capable of withstanding scrutiny in that environment (including the potential peer review of any proposed CBET). This means the considerations relating to possible satellite discoveries are rigorous; far more rigorous than in the processing of routine observations.

The assessment is in principle quite straight forward: establish that the only reasonable explanation for the observation is the existence of a satellite. Which means being able to exclude all other reasonably plausible explanations. Double stars and grazes are the most common alternative explanations, but not the only ones.

While it is open to anyone to undertake their own analysis and submit a proposed CBET for formal recognition, IOTA has a small group of people drawn from across the regions who are highly experienced in analysing occultation events, who undertake the analysis. This group has a well-established reputation with Central Bureau for Astronomical Telegrams (CBAT) [6] for the reliability of the analysis and results presented in a proposed CBET.

The analysis process involves team members critically reviewing the observation data, asking questions and requesting further information if needed. Inevitably there are times when difficult questions will be asked of the observer. This is an essential element of ensuring the reliability of a claim to a satellite; it is not a criticism of the observer. The final decision of the analysis is by consensus.

There are three possible outcomes from the analysis:

- **The observation is the detection of a satellite. All other possible explanations have been reasonably excluded**

This will lead to the drafting and submission of a CBET. The CBET will usually be drafted along the lines of 'F Flintstone (affiliation) reports the discovery of an apparent satellite of minor planet…',

with the observer being involved with the drafting. Submission may be undertaken by the observer if they desire, but it is usually done by a member of the analysis team to ensure CBAT is aware the analysis team has been involved with, and agrees with, the proposed CBET.

Within the *Occult* system the observation record will include the solution details for the satellite, and the CBET number that announces its discovery.

- **The observation could reasonably be explained by a satellite. However, there are other possible explanations that cannot be reasonably excluded**

No CBET will be prepared, nor a claim to a satellite discovery made. The observation record in *Occult* will include the possible satellite solution and an explanation about the status, with an observational status of 'Is it a satellite'.

For these events, it is highly desirable to have the 'possible satellite' status made public to those who are involved in measuring asteroid rotation light curves – so that they may make observations of the asteroid in the hope of confirming the existence of a satellite. This is best done in the Minor Planet Bulletin. A recent example is at page 163 of issue Vol. 53, No. 2 [7]. It is a one-page paper that that can be used as a template for writing such a paper. Importantly, if subsequently someone detects a satellite following from this publication, the fact of you making that publication should lead to you being treated as a co-discoverer.

Observers are encouraged to write and submit such papers. People on the analyst team will provide support when needed.

- **The observation is best explained by something other than a satellite**

The observation record in *Occult* will not include any satellite solution. In some situations, a 'Review flag' might also be set to facilitate retrieval of the event in the future. Depending on the circumstances, the record may include text to explain a satellite explanation was considered and excluded. Otherwise, it will be treated the same as any other single-body observation.

References

[1] Pavlov, H., Tangra software, http://www.hristopavlov.net/Tangra3/
[2] Stellar Occultation Data Input System (SODIS), https://sodis.iota-es.de/
[3] Herald, D., Occult software, http://www.lunar-occultations.com/iota/occult4.htm
[4] Pavlov, H. Occult Watcher desktop version, https://www.occultwatcher.net/
[5] Webpage of the Central Bureau for Astronomical Telegrams http://www.cbat.eps.harvard.edu/services/cbathist.html
[6] The 50 most recent CBETs, http://www.cbat.eps.harvard.edu/cbet/RecentCBETs.html
[7] Bao, V., Gault, D., A POTENTIAL NEW SATELLITE OF (165991) 2001 YL149 DETECTED BY STELLAR OCCULTATION, The Minor Planet Bulletin Vol. 53, No. 2, p. 163, https://mpbulletin.org/issues/MPB_53-2.pdf

The OLED Project - Lunar Occultations of Double Stars

Enrique Velasco · IOTA/ES · AAM[1] · Madrid · Spain · enriquevelasco349@gmail.com
Philippe Laurent · SAF[2] · Barjols · France · apilaure_astro@yahoo.fr
(1) Agrupación Astronómica de Madrid, (2) Société Astronomique de France

ABSTRACT: We present the OLED project (OLED = Occultations Lunaires d'Étoiles Doubles (fr) or Occultaciones Lunares de Estrellas Dobles (es)) to the IOTA community as a coordinated effort involving several dozen observers distributed across western and central Europe, with the goal to increase efforts to record lunar occultations of double stars. The project has been active for more than three years now and has so far collected over 600 contact measurements, including observations of both single and double stars. The reduction and analysis of these observations have already produced a substantial number of astrometric measurements. Our objective is to collect, analyse, and exploit these data to confirm stellar duplicity, derive accurate astrometric solutions, and contribute to orbital determination studies. The project is open to observers throughout Europe and worldwide, and seeks to revitalise lunar occultation observing, an area of renewed interest within IOTA/ES.

Introduction

Lunar occultations were once the core observational activity of IOTA from its very beginning, owing to their major practical and theoretical importance throughout the mid-20th century. They played a crucial role in establishing the uniform Ephemeris Time scale, improving the ephemerides of both the Moon and stars, and refining knowledge of the lunar limb.

As we know, interest in this field has gradually declined as a result of advances on several fronts. In particular, the introduction of the atomic-time-based UTC scale, the greatly improved accuracy of the lunar limb derived from lunar orbiter data, and the exceptional precision of modern lunar and stellar ephemerides obtained through planetary numerical integrations and astrometric missions such as Hipparcos and Gaia have reduced the scientific dependence on lunar occultations.

Accordingly, much of IOTA's activity has shifted toward the seemingly more productive field of asteroidal occultations, and there are strong reasons supporting this evolution.

However, despite these advances, the lunar occultation technique remains a powerful method for obtaining highly accurate astrometric measurements of the relative positions of double-star components, especially when multiple observations of the same system are collected by the same or different observers during one or several lunar occultation events.

From the late 2000s until quite recently, considerable effort was devoted within IOTA to promoting lunar occultation observations of double and multiple stars.

This initiative was led very successfully by the late Brian Loader, who served as a global coordinator for lunar occultation observations of double stars and strongly advanced this work worldwide. Following his retirement, however, the activity gradually declined and has since produced few tangible results.

The OLED Project

The OLED project [1], launched in 2022 through independent initiatives by SAF (Société Astronomique de France [2]) and AAM (Agrupación Astronómica de Madrid [3]) that were later unified into a single coordinated effort, can be regarded as a continuation of this earlier work. Initially focused on southwestern Europe, the project has the long-term goal of extending its coverage across a wider region of Europe and, eventually, to other parts of the world. The project is in line with IOTA interests, as recently advocated by our colleagues Alex Pratt and Konrad Guhl at ESOP XLIV [4], as well as by Oliver Klös [5] and Dietmar Büttner [6].

During its first three years of activity, the project has benefited greatly from the pioneering work of Herald, Gault, Loader, and several other key figures within IOTA. At the same time, we have carefully examined both historical and more recent professional studies in order to better understand the underlying concepts and assumptions involved in the reduction and interpretation of lunar occultation observations.

So far, the results have been encouraging. We therefore believe that the time has come to offer our infrastructure and experience to the wider IOTA community, with the hope of revitalising double star lunar occultation observations within both IOTA and the amateur astronomy community at large. Such a revival would be

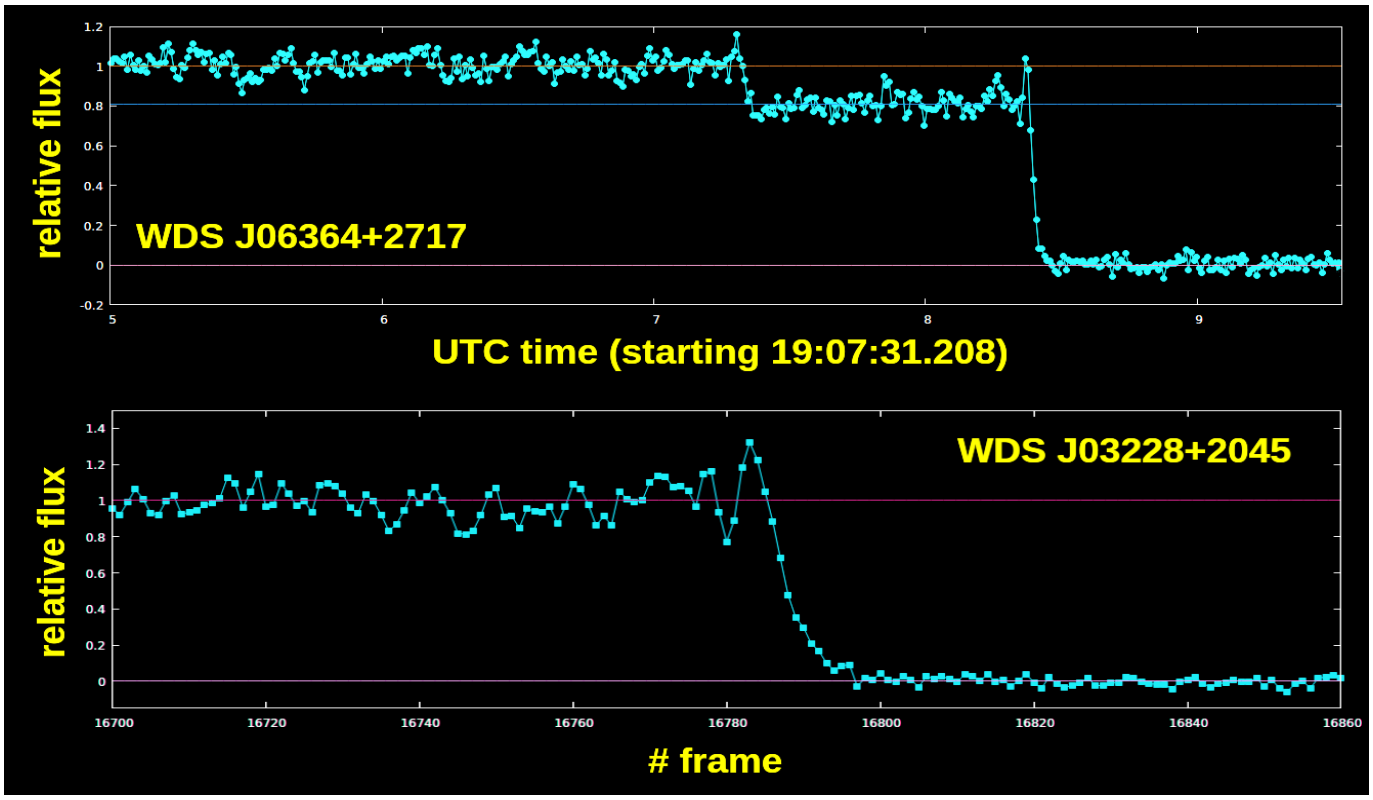

Figure 1. Two examples of visual-band light curves obtained during lunar occultations of double stars. Upper panel: A widely separated double star, WDS J06364+2717 , showing a clearly visible step, corresponding to a projected separation distance between components (absolute separation ρ=0.7", magnitude contrast Δm=1.8). Observation by P. Laurent (Barjols, France) at a frequency 100 Hz. Lower panel: Light curve of a close pair, WDS J03228+2045 (ρ=0.2", Δm=2.9), obtained at a sampling rate of 200 Hz. Observation by E. Velasco (Becerril de la Sierra, Spain). A subtle structure visible at the end of the diffraction ramp is produced by the secondary component. In both cases, diffraction effects are clearly visible, and the contact times must therefore be derived through fits to appropriate diffraction models.

especially valuable because, as in many other areas of occultation science, collaboration is essential for achieving meaningful results.

At present, about 25 observers contribute regularly to the OLED project. Most are based in Spain and France, with additional participants located in Germany and the United Kingdom.

The project is coordinated by the authors of this article. Observations are submitted in the form of processed light curves, using software such as *Tangra* [7], together with the observer's analysis of the contact times using *AOTA* or similar software, whenever such an analysis has been carried out. Otherwise, the analysis is performed by the coordinators. Two examples of light curves obtained by OLED observers are shown in Figure 1.

Aims of the Project

The main objectives of the project are the following.

- **Contact times and duplicity confirmation**
  We aim to collect and reduce contact-time measurements for both single and double stars, including systems known to be single as well as stars suspected of duplicity. We explore the zodiacal version of the Washington Double Star (WDS) catalogue [8] for known binary or multiple systems. Also, the Gaia DR3 NonSingle Star (NSS) catalogue [9] of unsolved orbital and accelerated stars is being used to schedule and observe their lunar occultations, in an effort to confirm its duplicity. It should be noted that, in the case of Gaia NSS stars, they are observed as a single unsolved source; however, lunar occultations make it possible to determine an updated position that confirms and refines the acceleration of their motions. The conclusions we can draw from these observations are currently being analysed.

- **Astrometry of double stars**
  Whenever possible, we derive one- (1D) or two-dimensional (2D) astrometric solutions from the observations, using methods pioneered by Nather and Evans [10] and Herald [11], although with several modifications intended to improve accuracy. In the 2D case both ρ and θ, the two astrometric parameters required to characterise the relative position of the secondary component with respect to the primary (Figure 2), can be determined. Obtaining a full 2D solution requires observations from at least two sufficiently separated observing stations.

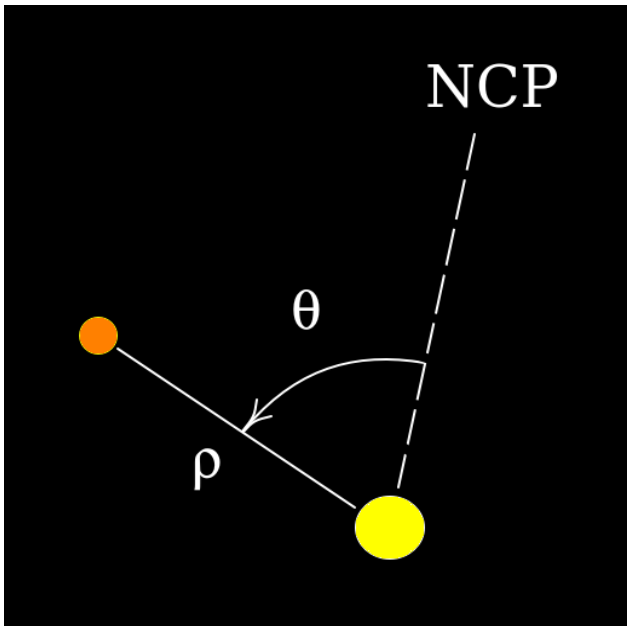

Figure 2. The two parameters defining the relative astrometry of a double star. ρ *represents the angular separation between the two components along the great circle connecting them. The parameter θ, the position angle, is defined as the angle between the celestial meridian passing through the primary star and the great circle joining the two components, measured eastward from the North Celestial Pole (NCP).*

In the case of a 1D solution, only a combination of the astrometric parameters can be derived, namely

$$\rho\,(a\cos\theta + b\sin\theta) = c,$$

where a, b, and c are constants determined from the lunar ephemeris and the local limb geometry. As a result, the possible values of ρ and θ are constrained, but cannot be uniquely determined. This situation occurs when the occultation is recorded from only a single observing site. Examples of 1D astrometric solutions are presented in Figure 3.

In this approach, the lunar limb only enters through an average limb slope. Although this limits the accuracy of the solution, the resulting uncertainties remain reasonable and controllable, provided that the separation ρ is not too large.

1D solutions obtained from different occultations of the same star can later be combined into a complete astrometric solution, provided that the observations are not too widely separated in time. However, in order to achieve a higher level of precision and fully exploit the current knowledge of the lunar limb profile, we employ a limb-projection technique that directly determines the stellar positions on the sky. From these reconstructed positions, the relative astrometry of the pair can then be derived. An example of this procedure is shown in Figure 4.

- **Orbit determination and refinement**

Another important aim of the project is to refine stellar orbits by combining previously published measurements from the WDS Catalogue with our own astrometric observations. Figure 5 presents an example of a successful orbit determination using OLED data.

At present, the orbits of only about 4,000 physically bound visual binary systems are known, according to the Sixth Catalog of Orbits of Visual Binary Stars (6Orb) [12]. Expanding our knowledge of binary-star orbits is therefore of high importance. Binary systems provide the most powerful, direct, and widely applicable method for determining the mass of a star, the fundamental physical parameter in stellar astrophysics.

This is achieved by measuring the relative position of one component of the pair (the secondary star) with respect to the other (the primary star) over a sufficiently long term interval, allowing the orbit of the system to be determined. Once the orbital parameters are known, Kepler's third law,

$$M_1+M_2=a^3/T^2,$$

can be applied to derive the total mass of the binary system. Here a is the semimajor axis (in astronomical units), T the period (in years), and the masses are expressed in units of solar mass.

1D solutions can also be used for orbit determination without the need to combine them with other similar solutions (which in many cases may be separated by very large intervals of time), because they still provide partial constraints on the orbital motion of the system. By combining these 1D measurements with complete astrometric positions, the orbital solution can be determined or refined. Consequently, even a single observation of a lunar-occultation event may provide scientifically valuable information. See [13] for a detailed discussion of this technique and a practical example.

Results: 2022 to Present

To date, a total of 580 contact measurements have been collected. Astrometric analyses have been carried out for 120 known double stars, yielding both one- and two-dimensional solutions. In addition, approximately 200 stars considered to be single have been observed in searches for possible duplicity or nonlinear motion on the sky. The latter may indicate stellar acceleration caused by an unresolved or invisible companion. Observations have also been obtained for a number of stars suspected of being double systems. Astrometric results are published in the journal *Étoiles Doubles* [14], a major reference source for European amateur double-star research, and are subsequently incorporated into the WDS Catalogue. The format and presentation of these reports is inspired by the style established by Brian Loader in his publications in the *Journal of Double Star Observations* [15].

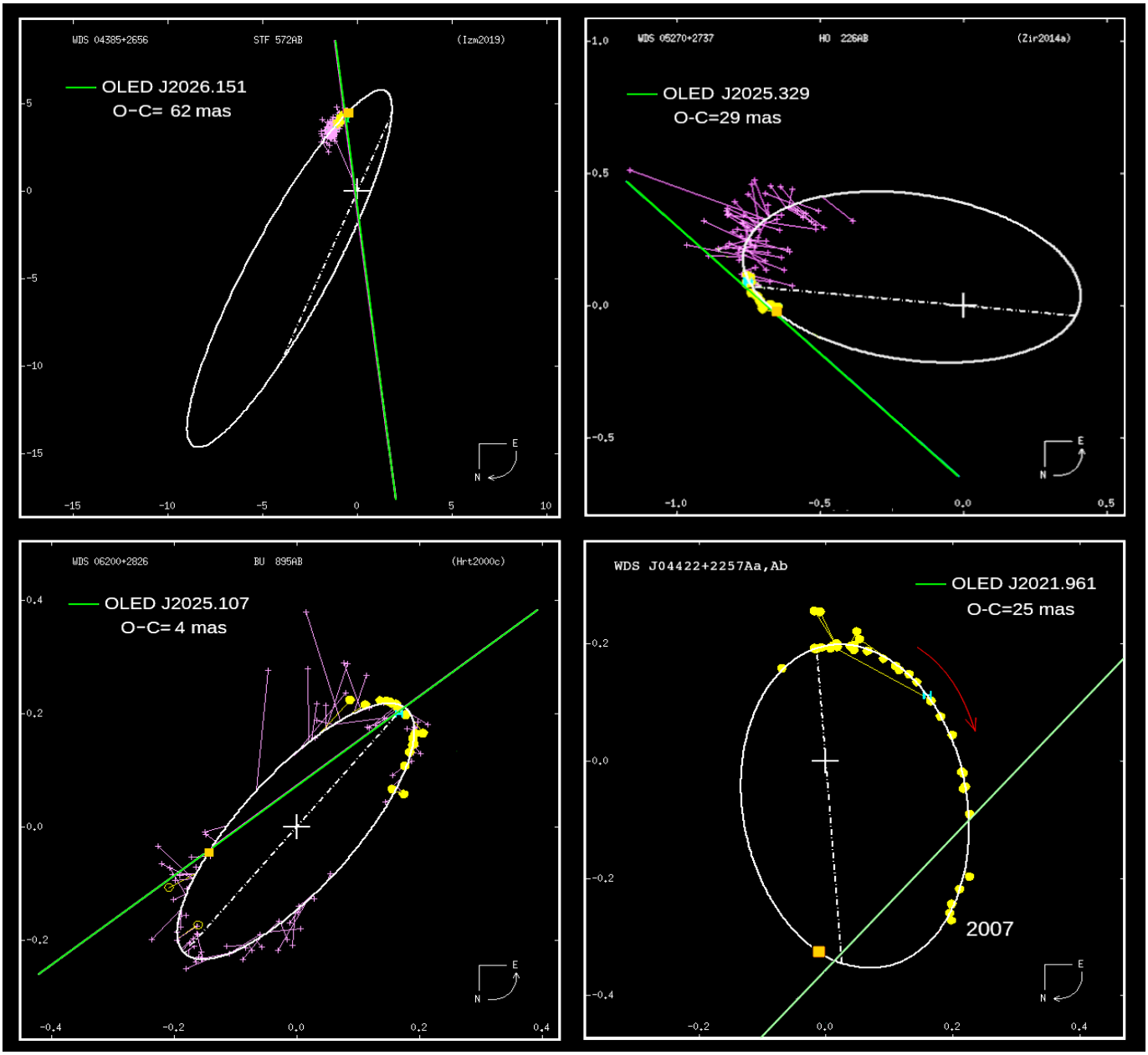

Figure 3. Several examples of one-dimensional (1D) astrometric solutions obtained within the OLED project. ***Upper left panel:*** *WDS J04385+2656. This system has a poorly determined grade-4 orbit, with available astrometric measurements covering only a short orbital arc. A lunar occultation recorded by a single observer, Rosendo Jorba (Caraquiz, Spain), allowed a 1D solution to be derived (green straight line). The orbital position predicted for the epoch of observation is indicated by the orange filled square. The observed-minus-calculated residual (O−C), defined as the distance between the predicted position and the 1D solution line, is 62 mas (milliarcseconds), significantly larger than the expected uncertainty of the measurement. This suggests that the current orbit may require substantial revision when additional astrometric data become available.* ***Upper right panel:*** *WDS J05270+2737, another system with a grade-4 orbit, observed by Ricard Casas (Catalonia, Spain). In this case, the residual is considerably smaller, possibly indicating that the published orbit is already reasonably close to the true solution.* ***Lower left panel:*** *WDS J06200+2826, a system with a well-determined grade-2 orbit. As expected, the residual of our observation, due to Javier de Elías (Majadahonda, Spain) is correspondingly very small, only 4 mas.* ***Lower right panel:*** *WDS J04422+2257Aa, Ab, a grade-3 orbit lacking recent astrometric observations. Our 1D solution, obtained from observations by E. Velasco (Becerril de la Sierra, Spain), at epoch J2021.961, approximately 15 years after the last available 2D measurement, leads to a recalculated orbit that remains close to the currently accepted solution, but with significantly smaller uncertainties in the orbital elements [13]. This demonstrates that 1D solutions can be extremely valuable and may sometimes play a role in orbit determination comparable to that of full 2D astrometric measurements. All graphs shown are modified versions of original diagrams extracted from the Sixth Catalog of Orbits of Visual Binary Stars (6Orb) [12].*

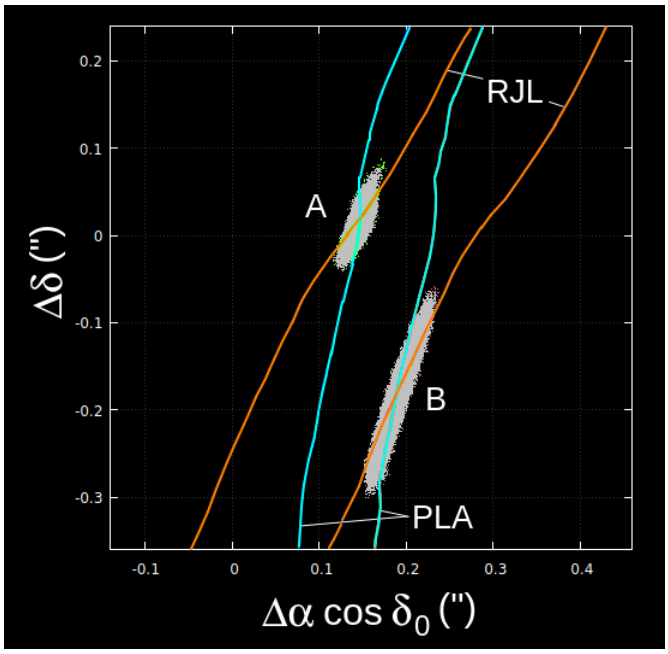

Figure 4. Sky-projected lunar limbs for the A and B components of the double star WDS J05017+2640AB (ρ=0.2", Δm=1.9). Intersection points from two observations obtained at different locations allow the absolute astrometric positions of each component to be determined, from which the relative position parameters of the star, ρ and θ, can be calculated. The origin of the diagram corresponds to the Gaia DR3 ICRS coordinates (α_0, δ_0) of the photocentre of the system, for which separate right ascension and declination values for the individual components are not available. The quantities Δα and Δδ represent offsets from this reference position. Lunar limb profiles were derived from LOLA data. The point clouds around the limb intersection points were generated through a Monte Carlo analysis and provide an estimate of the associated uncertainties. Observations by Ricard Casas (RJL) and Philippe Laurent (PLA).

A first report [16] was published in June 2024, providing extensive information on the project, the methods employed, and the results obtained. A second report has been prepared for publication in the June 2026 issue. A general introduction to the project can also be found in the same journal [17].

How to Contribute

At present, our strategy for organising the observing programme differs somewhat from that adopted in earlier IOTA double-star campaigns. Rather than maintaining an extensive list of suggested targets and waiting for observations of the same star from different occultation events to accumulate over time, we aim to maximise the likelihood of obtaining multiple observations of the same target within a shorter period. This approach increases the chances of deriving complete astrometric information at an earlier stage.

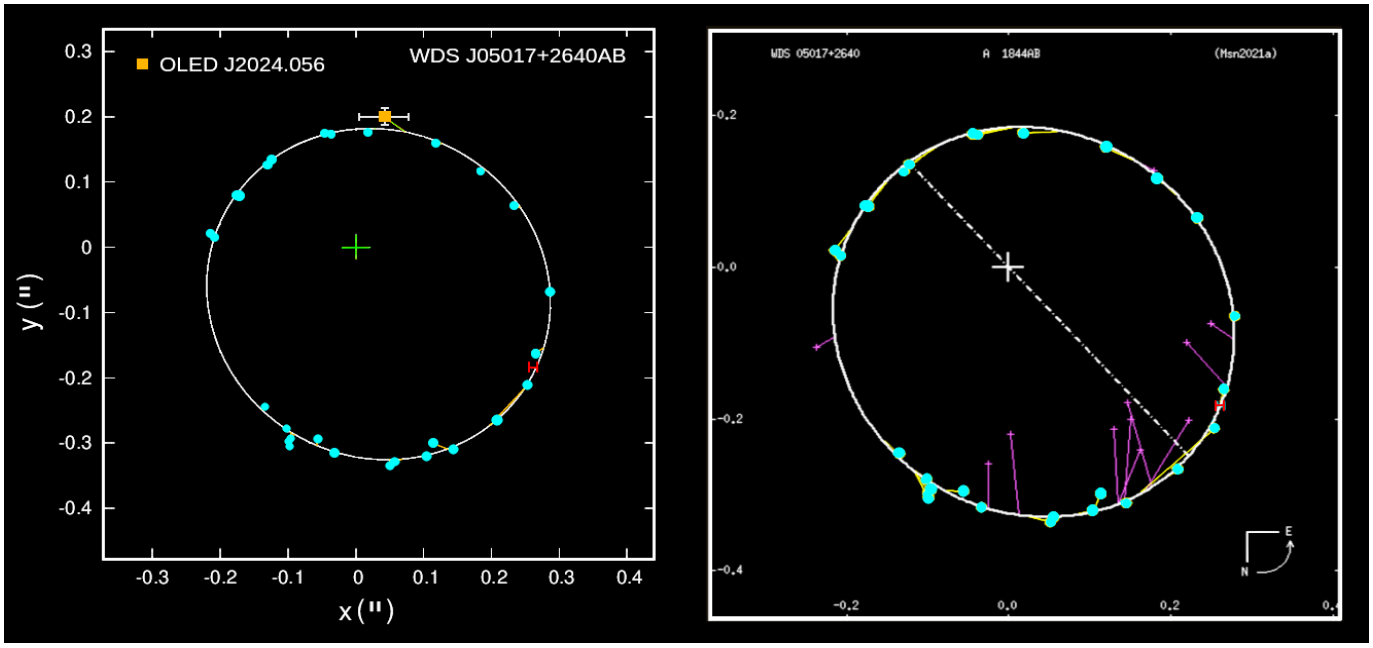

Figure 5. Astrometric measurements of WDS J05017+2640AB and orbit determination.
Left: New orbital solution incorporating previously published astrometric measurements together with the new position derived from the OLED astrometry shown in Figure 4 (E. Velasco, unpublished).
Right: Current orbital solution from the Sixth Catalog of Orbits of Visual Binary Stars (6Orb) [12]. The new OLED measurement at Julian epoch J2024.056 (displayed with estimated error bars) leads to a correction of the orbit, which is effectively rotated counterclockwise by a few degrees relative to the previous orbit. As a consequence, the total O-C residual is significantly reduced.
Astrometric measurements courtesy of Rachel Matson (USNO).

To achieve this, we publish a concise monthly target list, encouraging observers to concentrate their efforts on a selected set of stars. Nevertheless, observations of any double-star occultation are welcome, including events not included in the recommended monthly list.

Some observers prefer to schedule their observations using the *Occult* software rather than following our target lists. This approach is also perfectly acceptable, since in many cases the selected targets overlap with our own recommendations.

Personalised predictions are computed for participating observers and are also generated for major European cities. Observers interested in contributing are encouraged to submit their double-star occultation observations to one of the project coordinators.

A simple email is sufficient for submission, including a csv-file containing the photometric data together with a standard form specifying the observing location, equipment used, target star, and date of observation. At present, all information is submitted by email, although a dedicated web interface is currently under development to facilitate the submission process.

Conclusions

Continued monitoring of double stars remains essential, and the lunar-occultation technique provides access to the astrometry of both wide and close pairs, reaching angular resolutions of only a few tens of milliarcseconds, well beyond the capabilities of speckle interferometry or lucky-imaging techniques when used with amateur-sized telescopes. This remarkable capability arises from the relatively slow apparent motion of the Moon across the sky. With a typical angular velocity of about 0.4" per second, the lunar limb offers a highly favourable conversion factor between time measurements and angular separations, enabling extremely precise astrometric determinations from accurately timed occultation events.

Some amateur astronomers believe that the remarkable capabilities of *Gaia* have effectively brought stellar astrometry, and therefore double-star astrometry, to its conclusion, rendering lunar-occultation work obsolete or unproductive. However, although *Gaia* has surveyed an enormous number of resolved and unresolved binary systems, including stars with unseen companions, the mission itself has covered only a relatively short time span. Binary stars, most of which have orbital periods far longer than the duration of the *Gaia* mission, will continue to evolve dynamically for decades and centuries to come. Continued observations therefore remain essential. In this context, the lunar occultation technique continues to provide a simple yet remarkably powerful means of obtaining high-quality astrometric data that can support future orbital calculations. For amateur occultation observers, this is also a particularly accessible field of research. It requires precise time-stamping of observations, but inexpensive solutions are available, and observers of asteroid occultations who are interested in double stars are already well equipped. It generally does not require travel to specific geographic locations, numerous observable events occur every month and, perhaps most important, even modest individual contributions can significantly advance our understanding of double-star orbits and consequently of stellar astrophysics.

We express our sincere gratitude to all OLED observers for their contributions, which are essential to the continued success of this project.

References

[1] Homepage of the OLED Project
https://sites.google.com/aam.org.es/oled
[2] Homepage of Société Astronomique de France
https://saf-astronomie.fr/
[3] Homepage of Agrupación Astronómica de Madrid
https://www.aam.org.es/
[4] Klös, O., Pratt, A., ESOP XLIV - Report of the 44th European Symposium on Occultation Projects, Journal for Occultation Astronomy, 2025-4, p. 10-21 (2025), https://www.iota-es.de/JOA/JOA2025_4.pdf
[5] Klös, O., Lunar Occultations of Neglected Double Stars Brighter than 5 mag from the WDS, Journal for Occultation Astronomy, 2025-2, p. 3-8 (2025), https://www.iota-es.de/JOA/JOA2025_2.pdf
[6] Büttner, D., Lunar Occultation Observations – Former Developments – Current Situation – Future Prospects, Journal of Occultation Astronomy, 2025-2, p. 9-13 (2025), https://www.iota-es.de/JOA/JOA2025_2.pdf
[7] Pavlov, H., Tangra software, http://www.hristopavlov.net/Tangra3/
[8] The Washington Double Star Catalog, United States Naval Observatory (USNO), https://www.astro.gsu.edu/wds/
[9] Arenou, F. et al., Gaia Data Release 3. Stellar multiplicity, a teaser for the hidden treasure, *A&A* 674, A34 (2023), https://doi.org/10.1051/0004-6361/202243782
[10] Nather, R. E., and Evans, D. S., Photoelectric Measurement of Lunar Occultations. I. The Process, *Astron. J.* 75, 575 (1970), https://ui.adsabs.harvard.edu/scan/manifest/1970AJ.....75..575N
[11] Herald, D., SAO 97883 – a new double star, Journal of Double Star Observations Vol. 5 No. 4, 208-210 (2009), http://www.jdso.org/volume5/number4/Herald.pdf
[12] Matson, R. A. et al., Sixth Catalog of Orbits of Visual Binary Stars, https://www.astro.gsu.edu/wds/orb6.html
[13] Velasco, E., Orbits of binary stars from lunar occultations, Journal of Computational Astronomy and Astronomical Computing, 1, 15–24 (2024), https://federacionastronomica.es/images/web/Journal%20JCAAC/2024-nvbre/JCAAC_vol1.pdf
[14] Homepage of Étoiles Doubles, https://etoilesdoubles.org/
[15] Journal of Double Star Observations, https://doublestarsjournal.org/
[16] Velasco, E., Laurent; P. et al., "Project OLED - Lunar Occultations of Double Stars – Annual Report #1 (2021-2024)", *Étoiles Doubles* 8, p. 29-60 (2024), https://etoilesdoubles.org/revue/ED-2024-08/ED-2024-08-VELASCO.pdf
[17] Velasco, E. and Laurent, P., Project OLED: lunar occultations of double stars, *Étoiles Doubles* 7, p. 2-12 (2023), https://etoilesdoubles.org/revue/ED-2023-07/ED-2023-07-OLED.pdf

High-Speed Photometry of Lunar Occultations

Nikolai Wünsche · IOTA/ES · Biesenthal · Germany · nwuensche@astw.de

ABSTRACT: Observations of lunar occultations are back. Decades ago, they were the almost exclusive focus of occultation observers before losing much of their scientific importance. This is now about to change. Many modern cameras used in astronomy are capable of recording at very high frame rates. Now even non-paid astronomers can perform high-time-resolution photometry of these events. We are talking about 5 ms per frame or faster. At resulting frame rates of 200 fps and above, it is possible to observe diffraction effects and to detect and measure binary and multiple star systems. The OLED project (OLED = Occultations Lunaires d'Étoiles Doubles (FR) or Occultaciones Lunares de Estrellas Dobles (ES)) is the first in many years to scientifically analyse lunar occultation observations. Observing lunar occultations is back!

Introduction

Any observer of occultations by minor planets being frustrated by several 'negative' events in a row – that is, events with no measured occultation – should definitely take a look at the Moon: there are sometimes dozens of occultation events in a single night, and they are guaranteed to be 'positive'. Astrophotographers in particular need to rethink their approach – no wonder, as the goal *here* is just a single star and a high frame rate! This article can only serve as a brief overview. It is intended to offer a few tips and encourage you to try it out for yourselves.

Achieving High Frame Rates

The less data that needs to be transferred, the faster it is. Therefore, minimise the image size, the 'Region of Interest' (ROI), and do so drastically. I make the image area just small enough to fit the timestamp; an image height of 100 pixels is perfectly adequate. Reference stars are almost never present anyway, so a larger image area is useless. You can make the image even smaller than the timestamp, since the time is also encoded in the frame.

Hardware

- Camera

Cameras with an analogue video output are not suitable. Even older digital cameras with a small sensor and a USB 3 output or a FireWire 800 interface may be suitable. (Table 1).

Well suited	Less well suited
USB 3, Firewire IEEE 1394b ('FW 800')	USB 2
Monochrome camera	Colour camera
Small sensor, pixels of ~6 µm	
Global shutter	Rolling shutter
No cooling required	

Table 1. Comparison of digital cameras for high speed photometry of lunar occultations.

- Computer

- Fast computer (ample RAM and a fast SSD). Change your *Windows* Power Plan from "Balanced/Eco" to "High Performance". An energy-saving mode usually reduces processing power.

- Image capture software: Image capture software: Users of the DVTI+CAM [1] are advised to use the software supplied with the device. The manual includes guidance on, amongst other things, using a fixed ROI at high frame rates and avoiding dropped frames. For other cameras: the latest version of *SharpCap* [2] is recommended, as it is also ideally suited for high-speed photometry.

- Do not use USB 3 extension cables. Instead, place the PC close to the telescope.

Camera Settings

- Use the "ADV" video format. The "SER" video format should generally not be used [3]. With FITS images, speed issues arise at high frame rates when several hundred files need to be stored per second.

- Monochrome

- Use 12-bit, 14-bit or 16-bit: Although this generates more data than 8-bit, the photometric resolution is much better and you can also measure small steps in magnitude.

- 2x2 binning: This increases the camera's apparent sensitivity, allowing you to measure fainter stars at a high frame rate.

- USB Traffic (QHY), USB Speed (ZWO): This is a particularly sensitive parameter. Keep the 'USB Traffic' as close to zero as possible to achieve the best frame rate with a QHY camera. In contrast, the 'USB Speed' setting for ZWO cameras must be set to a high value. Taking into

account the selected parameters for field of view, exposure time, bit rate and binning, you must adjust the USB traffic or USB speed so that no more frames are lost, whilst ensuring that the displayed number of 'fps' (frames per second) does not drop too much.

Please note that the optimal USB traffic/speed setting can only be achieved with a specific configuration (ROI, frame rate, etc.) for your particular setup. There's no rule such as 'my friend always uses value X' and that will work for you too. You'll need to try it out for your system, make a note of it and apply it.

It is worth trying all the USB 3 ports on the PC: they are sometimes connected to different points in the system and have varying speeds.

As with all occultation observations, the following applies:

Do not measure stars that are too faint or use too high a frame rate. Gain should not be set too high, as this will cause excessive noise. In the end, a very noisy light curve cannot be analysed and you've simply wasted your time.

Observation Duration

Predictions for lunar occultations are very accurate – if they are calculated for your observation site. Calculate your own predictions using the software *Occult* [4] or *GRAZPREP* [5]. Usually, it is sufficient to start recording 20 seconds before the event and stop 5–10 seconds after it.

Take care with known binary stars: the prediction often specifies the midpoint of the occultations of the separate components.

Measuring Time with Cameras without GPS

In the specific task of 'measuring multiple star systems with lunar occultations', there is less need to measure events with absolute accuracy to within a few milliseconds. Without a GPS timestamp, this would be a challenge. It is more important to measure the individual data points with relative accuracy in relation to one another. To achieve this, the frames must be recorded consistently and without any gaps.

For cameras without a GPS module, NTP with Meinberg software [6] is sufficient as a time reference. For more details, refer to [7].

Checking the Configuration

You should make a test recording of the star for a few seconds (~1000 frames) using the configuration found and then, for example, use *DVTI Video Tools* [8] to check at random that the frames have indeed been written regularly, i.e. whether the timestamps follow each other evenly, with the interval between them only slightly greater than the exposure time, and whether there are no jumps or gaps in time.

If not, reduce the frame rate by increasing the integration time. If there are dropped frames, also increase the value for 'USB traffic'.

This check can also be carried out using software like *Tangra/AOTA* [9, 4] or *PyMovie/PyOTE* [10], which would display dropped frames as well as errors in the timestamps.

Conclusion

Observations like these will immerse you in the world of milliarcseconds. You'll be amazed by the results. A possible next step would be to use narrowband filters to produce defined diffraction patterns. Finally, the results must be reported; in this case, to two recipients: the respective local coordinator for Lunar occultations – and, of course, to the OLED project [11, 12] which uses the high-speed photometry data for its research (see the article 'The OLED Project – Lunar Occultations of Double Stars' in this issue.

I hope the articles in this issue have inspired you to observe lunar occultations with high-speed photometry by yourself.

References

[1] Schweizer, A., Meister, S., DVTI+CAM, webpage, https://dvticam.com
[2] Glover, R., SharpCap software, https://www.sharpcap.co.uk/
[3] Pavlov, H. et al., The Astronomical Digital Video (ADV) Data Format, Journal for Occultation Astronomy, Vol. 10, No. 3, p. 8-12, https://www.iota-es.de/JOA/JOA2020_3.pdf
[4] Herald, D., Occult/AOTA software, http://www.lunar-occultations.com/iota/occult4.htm
[5] Riedel, E., GRAZPREP software, http://www.grazprep.com/
[6] Meinberg software for Windows, https://www.meinbergglobal.com/english/sw/#win
[7] Wünsche, N., Time measurement on Windows, IOTA/ES webpage, https://www.iota-es.de/guidelines/Time_measurement.pdf
[8] Schweizer, A., Meister, S., DVTI Video Tools software, https://dvticam.com/support/
[9] Pavlov, H., Tangra software, http://www.hristopavlov.net/Tangra3/
[10] Anderson, B., PyMovie/PyOTE software, https://occultations.org/observing/software/pymovie/
[11] Homepage of the OLED project: https://sites.google.com/aam.org.es/oled/
[12] Monthly updated observation programme of OLED project: https://astro-oled.es/oled/

Beyond Jupiter

The World of Distant Minor Planets

Since the downgrading of Pluto in 2006 by the IAU, the planet Neptune marks the end of the zone of planets. Beyond Neptune, the world of icy large and small bodies, with and without an atmosphere (called Trans-Neptunian Objects or TNOs) starts. This zone between Jupiter and Neptune is also host to mysterious objects, namely the Centaurs and the Neptune Trojans. All of these groups are summarised as "distant minor planets". Occultation observers investigate these members of our solar system, without ever using a spacecraft. The sheer number of these minor planets is huge. As of 2026 June 30, the *Minor Planet Center* listed 2233 Centaurs and 4058 TNOs.

In the coming years, JOA wants to portray a member of this world in every issue; needless to say not all of them will get an article here. The table shows you where to find the objects presented in former JOA issues. (KG)

No.	Name	Author	Link to Issue
944	Hidalgo	Oliver Klös	JOA 1 2019
2060	Chiron	Mike Kretlow	JOA 2 2020
5145	Pholus	Konrad Guhl	JOA 2 2016
5335	Damocles	Oliver Klös	JOA 2 2023
7066	Nessus	Konrad Guhl	JOA 1 2024
8405	Asbolus	Oliver Klös	JOA 3 2016
10370	Hylonome	Konrad Guhl	JOA 3 2021
10199	Chariklo	Mike Kretlow	JOA 1 2017
15760	Albion	Nikolai Wünsche	JOA 4 2019
15810	Awran	Konrad Guhl	JOA 4 2021
20000	Varuna	Andre Knöfel	JOA 2 2017
28728	Ixion	Nikolai Wünsche	JOA 2 2018
31824	Elatus	Konrad Guhl	JOA 2 2025
32532	Thereus	Konrad Guhl	JOA 1 2023
38628	Huya	Christian Weber	JOA 2 2021
47171	Lempo	Oliver Klös	JOA 4 2020
49036	Pelion	Joachim Siegert	JOA 4 2025
50000	Quaoar	Mike Kretlow	JOA 1 2020
53311	Deucalion	Konrad Guhl	JOA 2 2024
54598	Bienor	Konrad Guhl	JOA 3 2018
55576	Amycus	Konrad Guhl	JOA 1 2021
58534	Logos & Zoe	Konrad Guhl	JOA 4 2023

In this Issue:

(52975) Cyllarus

Michael O'Connell · IOTA/ES · BAA · Kildare · Republic of Ireland · michaeloconnell78@gmail.com

ABSTRACT: (52975) Cyllarus is a Centaur object discovered in 1998 by the SPACEWATCH® program at Kitt Peak Observatory. With a period of 134 years, it follows a highly eccentric (e = 0.377) and moderately inclined orbit (12.6°), placing it in the vicinity of both Uranus and Neptune. (52975) Cyllarus exhibits a very red surface (B-R= 1.81), indicative of complex organic materials common among primitive outer solar system bodies, and has an estimated diameter of ~56 km. Its rotation, shape, and activity remain unknown, and no stellar occultations have yet been observed, though a potential event is predicted for 2031, highlighting the need for improved astrometry.

No.	Name	Author	Link to Issue
60558	Echeclus	Oliver Klös	JOA 4 2017
65489	Ceto and Phorcys	Konrad Guhl	JOA 1 2025
90377	Sedna	Mike Kretlow	JOA 3 2020
90482	Orcus	Konrad Guhl	JOA 3 2017
120347	Salacia	Andrea Guhl	JOA 4 2016
121725	Aphidas	Konrad Guhl	JOA 1 2026
134340	Pluto	Andre Knöfel	JOA 2 2019
136108	Haumea	Mike Kretlow	JOA 3 2019
136199	Eris	Andre Knöfel	JOA 1 2018
136472	Makemake	Christoph Bittner	JOA 4 2018
174567	Varda	Christian Weber	JOA 2 2022
208996	2003 AZ_8	Sven Andersson	JOA 3 2022
225088	Gonggong	Mike Kretlow	JOA 2 2026
229762	G!kún‖'hòmdímà	Konrad Guhl	JOA 3 2025
341520	Mors-Somnus	Konrad Guhl	JOA 4 2022
471143	Dziewanna	Wojciech Burzyński	JOA 3 2024
486958	Arrokoth	Julia Perła	JOA 3 2023
–	2004 XR_{190}	Carles Schnabel	JOA 1 2022
541132	Leleākūhonua	Konrad Guhl	JOA 4 2024

The Discovery

Centaur asteroids are small celestial bodies that orbit the Sun in the outer regions of the solar system, typically between Jupiter and Neptune. They are considered transitional objects because they share characteristics of both asteroids and comets: some are like rocky asteroids while others are like comets which can develop a coma or tail as they move closer to the Sun. Centaurs are thought to originate from the Kuiper Belt and are often dynamically unstable, meaning their orbits can change significantly over relatively short astronomical timescales due to gravitational interactions with the giant planets. Studying Centaur asteroids helps astronomers understand the evolution of the solar system and the processes that move objects from the outer solar system into the inner regions.

(52975) Cyllarus was discovered on 1998 Oct 12. by N. Danzal at the *Steward Observatory*, Kitt Peak, Arizona, USA (IAU Code 691) [1]. This observatory houses the 0.9m (36-inch) SPACEWATCH® Newtonian telescope [2]. With an initial designation of 1998 TF_{35} and a magnitude estimate of 22.5 V, it was first reported by the Minor Planet Center on 1999 June 22 [3]. It was formally assigned the asteroid number (52975) on 2003 June 14 [1]

The Name

In Greek mythology, centaurs are creatures with the upper body of a human and the lower body of a horse, symbolising the conflict between civilisation and untamed nature. They were known for their wild behaviour, strong passions, and love of wine, while often living in forests and mountains far from human society. While most centaurs were seen as violent, some stood out for their wisdom, nobility, and skills in medicine, music, and teaching. Through these contrasting traits, centaurs represented the dual nature of humanity, balancing reason and instinct.

Figure 1. Relief depicting Cyllarus and his lover Hylonome (Credit: Classic Art Research Centre, University of Oxford) (Source: https://www.beazley.ox.ac.uk/record/937B735D-A895-4C88-BB9B-7518FD8359FE)

(52975) Cyllarus is named for a centaur who was mortally injured by a spear in battle. During the conflict with the Lapiths, he was struck by a javelin, prompting his lover Hylonome to rush to him and cradle his head as he died. Although Hylonome survived the brutal fighting, her grief proved unbearable, and she ultimately took her own life [4].

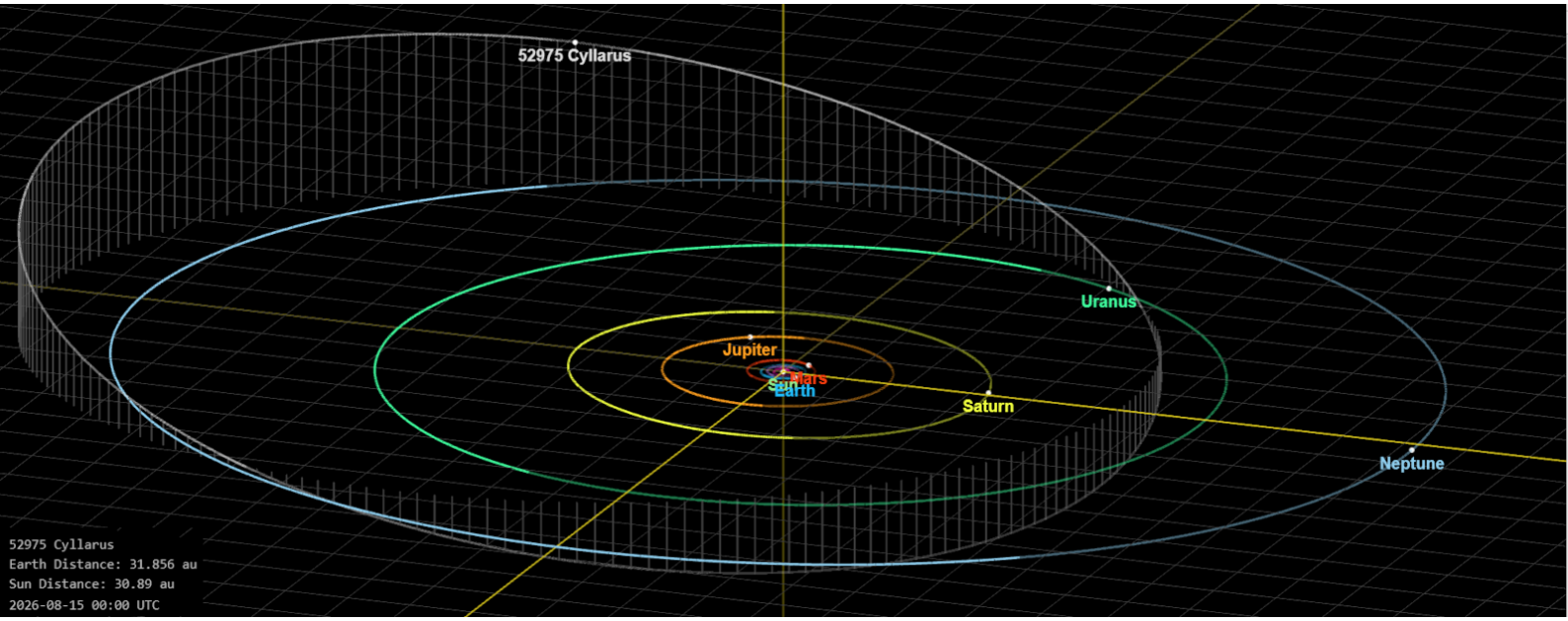

Figure 2. Orbit diagram and position of (52975) Cyllarus on 2026 August 15. (Source: https://ssd.jpl.nasa.gov/tools/sbdb_lookup.html#/?sstr=52975&view=VOP)

The Orbit

The orbit has a strong eccentricity of 0.377 and is inclined to the ecliptic by 12.6° (Figure 2). The object's distance from the Sun currently varies between 16.4 au (inside the orbit of Uranus) to 36.2 au (outside the orbit of Neptune) [5] and is therefore classified as a Centaur. Due to the combination of its relatively high inclination and pronounced eccentricity, (52975) Cyllarus can never collide with either planet. The next perihelion is calculated to occur in 2125. The current distance from the Sun (Epoch 2026.5) is 30.82 au.

The Physical Characteristics

(52975) Cyllarus is very red in colour with a B-R of 1.81 [6]. This suggests a surface rich in complex organic compounds (tholins) formed when ices containing carbon, nitrogen, and methane are altered by long-term exposure to solar radiation and cosmic rays. Such red surfaces are common among Centaurs and Kuiper Belt objects, supporting the conclusion that (52975) Cyllarus belongs to this primitive outer-solar-system population [7].

While often quoted as having a diameter of 62 km, the latest published data indicates a diameter of 56 km (+21 / -18 km) [8]. Notwithstanding the imaging efforts to date, its rotational period and detailed shape remain unknown as no rotational lightcurve has been published. Furthermore, there is no evidence of cometary activity to date.

Future Occultations

Thus far, there have been no confirmed observations of occultations involving this body. Using Dave Herald's *Occult* software [9], we find a prediction for a potential stellar occultation event in 2031 (Figure 3). This event involves occulting the +12.9 mag star UCAC4 591-047384 in 2031 Feb 03. While the centreline of the event is currently off the path of Earth, a significant error margin in this shadow path remains, so it may be visible over the Americas. The predicted path's error margin is due to the limited number of observations to date, and so more astrometry is required to confirm an accurate occultation shadow path.

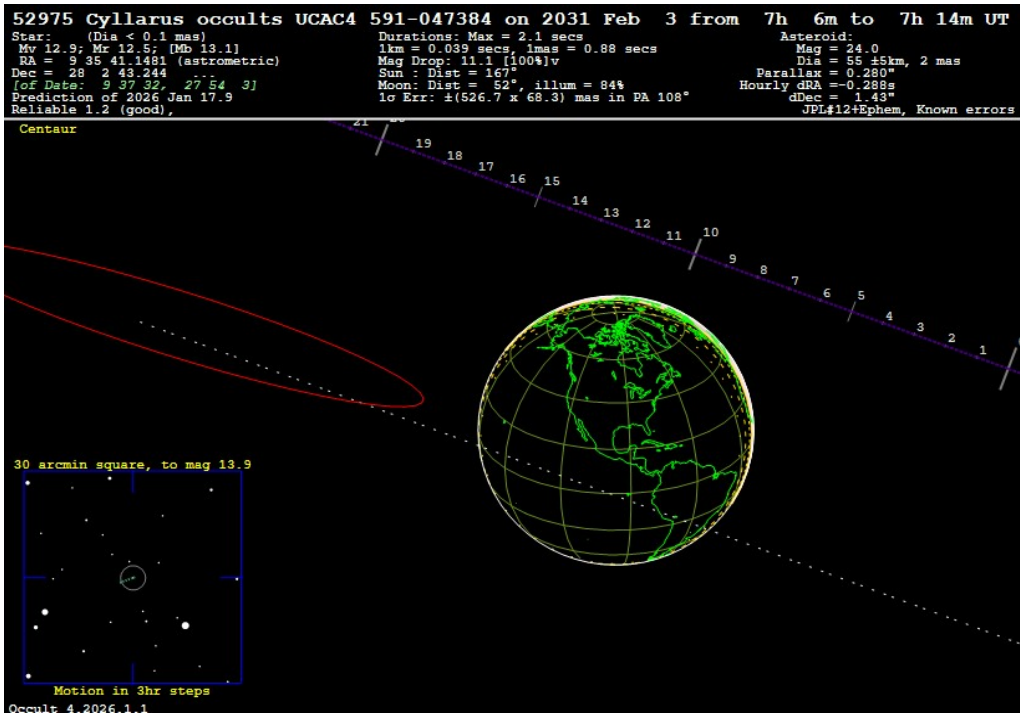

Figure 3. Map of the predicted path of the occultation on 2031 February 03 (Occult V4.2026.1.1).

References

[1] Minor Planet Circular 49102
https://www.minorplanetcenter.net/iau/ECS/MPCArchive/2003/MPC_20030614.pdf

[2] The University of Arizona – SPACEWATCH ® 0.9-metre Telescope
https://spacewatch.lpl.arizona.edu/telescopes#09meter

[3] Minor Planet Supplement MPS 4828
https://www.minorplanetcenter.net/iau/ECS/MPCArchive/1999/MPS_19990622.pdf

[4] Ovid (8), "*Metamorphoses*" Book XII, Lines 392-428, tr. A.S. Kline
https://ovid.lib.virginia.edu/trans/Metamorph12.htm

[5] Asteroids - Dynamic Site (AstDyS-2)
https://newton.spacedys.com/astdys/index.php?pc=1.1.1&n=52975

[6] Wm. Robert Johnston (2025), List of known trans-Neptunian objects and Centaurs, https://www.johnstonsarchive.net/astro/tnoslist.html

[7] Delsanti, A. et al. (2004), Simultaneous visible-near IR photometric study of Kuiper Belt Object surfaces with the ESO/Very Large Telescopes. Astronomy & Astrophysics 417, 1145–1158
https://www.aanda.org/articles/aa/pdf/2004/15/aa0182.pdf

[8] Duffard, R. et al. (2014), "TNOs are Cool": A survey of the trans-Neptunian region. XI. A Herschel-PACS view of 16 Centaurs. Astronomy & Astrophysics 564, A92
https://www.aanda.org/articles/aa/pdf/2014/04/aa22377-13.pdf

[9] Herald, D. (2026): Occult v4.2026.1.1 software tool
http://www.lunar-occultations.com/iota/occult4.htm

News

2026 IOTA\RECON Annual Meeting, Longmont, Colorado, USA, July 17-19, and (5232) Jordaens Occultation, July 20/21

The 2026 Annual Meeting of the International Occultation Timing Association (IOTA) will be held jointly with RECON (Research and Education Collaborative Occultation Network) in Longmont, Colorado, USA, 50 km north of Denver, on 2026 July 18 and 19.

It will feature preparations for, and observing, the occultation of 13.6 mag star UCAC4 424-071654 by the binary asteroid (5232) Jordaens on July 21 4h 29m UTC (that's Monday, July 20 at 10:29pm MDT). Recent analysis of *Gaia* data, combined with the 2024 satellite discovery from an occultation (CBET 5382) shows that we can predict the location of the satellite relative to the main body well enough that, with multiple observers, we can obtain good astrometric positions of both objects, and better characterise the primary body.

During the evenings, weather permitting, starting Friday July 17, there will be practice observing sessions at Marc Buie's large property in Longmont, using RECON or your own equipment; there should be enough of the former if you can't, or don't want to, bring your own gear. The Monday evening (5232) Jordaens occultation path passes not far east of Longmont, as shown in Figure 1.

As has been done in the past, the meeting will be both in person and virtual. Some observers not at the meeting in person plan to try to observe the (5232) Jordaens event from other locations along the path; they will coordinate coverage with the meeting observers. By the time this is published, more details, including a preliminary schedule and information about a planned block of motel rooms in Longmont that will be reserved for participants, will be posted on IOTA's website at:

https://occultations.org/community/meetingsconferences/na/2026-iota/

Webpage of RECON: https://tnorecon.net/

(D. Dunham, IOTA)
(J. Keller, RECON)

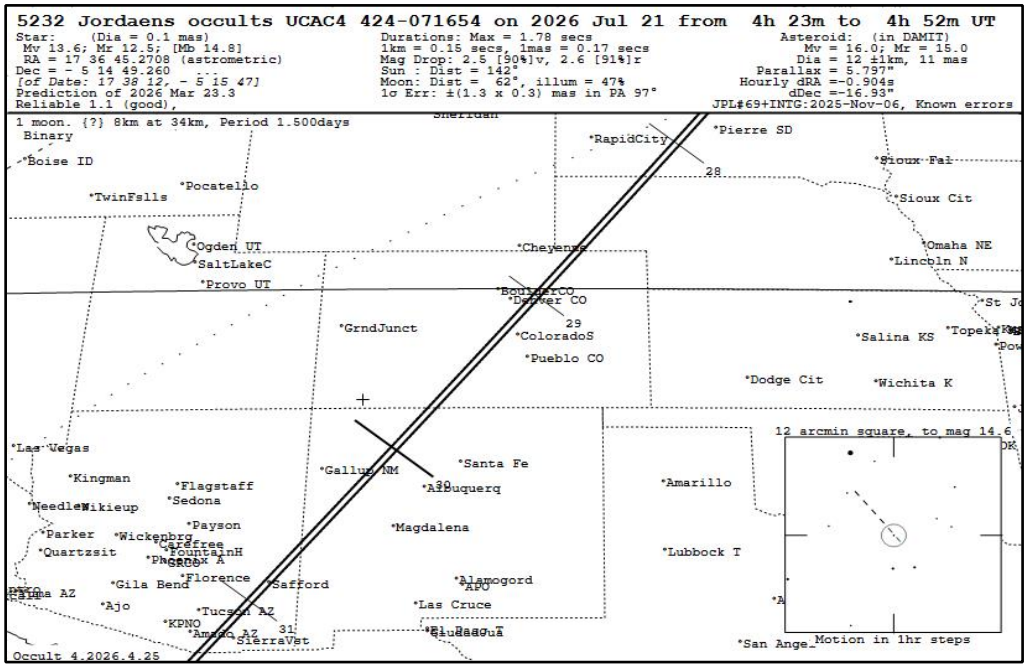

Figure 1. Occult map showing the path of the July 21st (UT) occultation by (5232) Jordaens across the central USA. (Occult V4.2026.4.25)

News

Invitation to the IOTA/EA FY2026/27 Annual General Meeting

The International Occultation Timing Association/East Asia (IOTA/EA) will hold the FY2026/27 Annual General Meeting on 2026 August 30 from 01:00 to 07:00 UT. The meeting will be held via interactive remote access via Zoom and simultaneous streaming via YouTube. Anyone can watch the YouTube streaming.

The meeting will include the agenda with voting by the full membership. In addition, there will be presentations by participants. A break of one hour is scheduled in the middle of the sessions.

Presentations may be given by non-members of IOTA/EA. The content of the presentation should focus on occultation predictions, observations, related activities and research using occultation phenomena in a broad sense. The duration of each presentation will be 15 minutes + 5 minutes for Q&A, but durations may be changed depending on the number of presentations. Oral presentations can be made in any language. It is recommended that slides be prepared in English. Please submit your presentations by 2026 August 10.

A special form will be available on the IOTA/EA website for attending the Annual General Meeting, accepting presentations, and accepting powers of attorney. Please register for your participation. The maximum number of participants is 80. Participation is open to all, whether members or nonmembers, but members will be given priority if the number of participants exceeds the limit.

Schedule and Deadlines (tentative):

- 2026 July 01: Registration opens
- 2026 August 10: Deadline for submitting presentations
- 2026 August 28: Deadline for registration

Please check the webpage of IOTA/EA for details and latest news:

https://www.perc.it-chiba.ac.jp/iota-ea/wp/

(O. Klös, IOTA/EA Circular 2026-06-01)

New Asteroid Satellite Discoveries Announced on CBET

The chase for satellites of asteroids goes on. The Central Bureau for Astronomical Telegrams has announced the following discoveries since the last issue of JOA:

- (1045) Michela, 2025 Oct 09,
  C. McPartlin, CBET 5685

- (12148) Caravaggio, 2026 Jan 27,
  J.-F. Gout, CBET 5679

- (40724) 1999 SY_8, 2026 Feb 10,
  B. Whitehurst, D. Sailing, CBET 5697

- (130247) 2000 CE_{85}, 2026 Mar 05,
  G. Viscome, D. Benjamin, CBET 5683

- (92590) 2000 PT_{13}, 2026 Mar 07,
  P. Maley, CBET 5686

- (3619) Nash, 2026 Apr 28,
  L. Benedyktowicz, D. Błażewicz, CBET 5691

- (134717) 2000 AO_1, 2026 May 10,
  W. Pieczonka, D. Błażewicz, CBET 5706

- (223393) 2003 SD_{106}, 2026 May 12,
  M. Skrutskie, CBET 5709

Access to the 50 most recent CBETs is available here:

http://www.cbat.eps.harvard.edu/cbet/RecentCBETs.html

(O. Klös)

Journal for Occultation Astronomy

IOTA's Mission

The International Occultation Timing Association, Inc was established to encourage and facilitate the observation of occultations and eclipses It provides predictions for grazing occultations of stars by the Moon and predictions for occultations of stars by asteroids and planets, information on observing equipment and techniques, and reports to the members of observations made.

The Journal for Occultation Astronomy (JOA) is published on behalf of IOTA, IOTA/ES and RASNZ and for the worldwide occultation astronomy community.

Worldwide Partners

Club Eclipse (France). . . . . www.astrosurf.com/club_eclipse
IOTA/EA (East Asia) . . . . . https://www.perc.it-chiba.ac.jp/iota-ea/wp/
IOTA-India . . . . . http://iota-india.in
IOTA/ME (Middle East) . . . . . www.iota-me.com
President: Atila Poro . . . . . iotamiddleeast@yahoo.com
LIADA (Latin America) . . . . . www.ocultacionesliada.wordpress.com
SOTAS (Stellar Occultation Timing Association Switzerland) . . . . . www.occultations.ch

Imprint

Publisher: International Occultation Timing Association/European Section e.V.
Am Brombeerhag 13, D-30459 Hannover, Germany
Responsible in Terms of the German Press Law (V.i.S.d.P.): Konrad Guhl
Editorial Board: Wolfgang Beisker, Oliver Klös, Alexander Pratt, Carles Schnabel, Christian Weber
Contact:joa@iota-es.de
Layout Artist: Oliver Klös Webmaster: Wolfgang Beisker
JOA Is Funded by Membership Fees (Year): IOTA: US$15.00 IOTA/ES: €20.00 RASNZ: NZ$35.00
Publication Dates: 4 times a year

Submission Deadline for JOA 2026-4: September 15

IOTA maintains the following web sites for your information and rapid notification of events:

www.occultations.org
www.iota-es.de
www.occultations.org.nz

These sites contain information about the organisation known as IOTA and provide information about joining.

The main page of occultations.org provides links to IOTA's major technical sites, as well as to the major IOTA sections, including those in Europe, East Asia, Middle East, Australia/New Zealand, and South America.

The technical sites hold definitions and information about all issues of occultation methods. It contains also results for all different phenomena. Occultations by the Moon, by planets, asteroids and TNOs are presented. Solar eclipses as a special kind of occultation can be found there as well results of other timely phenomena such as mutual events of satellites and lunar meteor impact flashes.

IOTA and IOTA/ES have an on-line archive of all issues of Occultation Newsletter, IOTA'S predecessor to JOA.

Journal for Occultation Astronomy
(ISSN 0737-6766) is published quarterly in the USA by the International Occultation Timing Association, Inc. (IOTA)
PO Box 20313, Fountain Hills, AZ 85269-0313
IOTA is a tax-exempt organization under sections 501(c)(3) and 509(a)(2) of the Internal Revenue Code USA, and is incorporated in the state of Texas. Copies are distributed electronically.

Regulations

The Journal for Occultation Astronomy (JOA) is not covenanted to print articles it did not ask for.

The author is responsible for the contents of his article & pictures.

If necessary for any reason JOA can shorten an article but without changing its meaning or scientific contents.

JOA will always try to produce an article as soon as possible based to date & time of other articles it received – but actual announcements have the priority!